10 Yanagi Y, Ono N, Tatsuo H, Hashimoto K, Minagawa H: Measles virus receptor SLAM (CD150). Virology 2002;299:155–161.
11 Bartz R, Brinckmann U, Dunster LM, Rima B, ter Meulen V, Schneider-Schaulies J: Mapping amino acids of the measles virus hemagglutinin responsible for receptor (CD46) downregulation. Virology 1996;224:334–337.
12 Lecouturier V, Fayolle J, Caballero M, Carabaña J, Celma ML, Fernandez-Muñoz R, Wild TF, Buckland R: Identification of two amino acids in the hemagglutinin glycoprotein of measles virus (MV) that govern hemadsorption, HeLa cell fusion, and CD46 downregulation: phenotypic markers that differentiate vaccine and wild-type MV strains. J Virol 1996;70:4200–4204.
13 Takeda M, Kato A, Kobune F, Sakata H, Li Y, Shioda T, Sakai Y, Asakawa M, Nagai Y: Measles virus attenuation associated with transcriptional impediment and a few amino acid changes in the polymerase and accessory proteins. J Virol 1998;72:8690–8696.
14 Hsu EC, Sarangi F, Iorio C, Sidhu MS, Udem SA, Dillehay DL, Xu W, Rota PA, Bellini WJ, Richardson CD: A single amino acid change in the hemagglutinin protein of measles virus determines its ability to bind CD46 and reveals another receptor on marmoset B cells. J Virol 1998;72:2905–2916.
15 Xie M, Tanaka K, Ono N, Minagawa H, Yanagi Y: Amino acid substitutions at position 481 differently affect the ability of the measles virus hemagglutinin to induce cell fusion in monkey and marmoset cells co-expressing the fusion protein. Arch Virol 1999; 144:1689–1699.
16 Nielsen L, Blixenkrone-Møller M, Thylstrup M, Hansen NJ, Bolt G: Adaptation of wild-type measles virus to CD46 receptor usage. Arch Virol 2001;146:197–208.
17 Erlenhofer C, Duprex WP, Rima BK, ter Meulen V, Schneider-Schaulies J: Analysis of receptor (CD46, CD150) usage by measles virus. J Gen Virol 2002;83:1431–1436.
18 Schneider-Schaulies S, Schneider-Schaulies J, Niewiesk S, ter Meulen V: Measles virus: immunomodulation and cell tropism as pathogenicity determinants. Med Microbiol Immunol 2002;191:83–87.
19 Rima BK, Earle JA, Baczko K, ter Meulen V, Liebert UG, Carstens C, Carabana J, Caballero M, Celma ML, Fernandez-Munoz R: Sequence divergence of measles virus haemagglutinin during natural evolution and adaptation to cell culture. J Gen Virol 1997; 78:97–106.
20 Li L, Qi Y: A novel amino acid position in hemagglutinin glycoprotein of measles virus is responsible for hemadsorption and CD46 binding. Arch Virol 2002;147:775–786.
21 Nielsen L, Andersen MK, Jensen TD, Blixenkrone-Møller M, Bolt G: Changes in the receptor binding haemagglutinin protein of wild-type morbilliviruses are not required for adaptation to Vero cells. Virus Genes 2003;27:157–162.
22 Seki F, Takeda M, Minagawa H, Yanagi Y: Recombinant wild-type measles virus containing a single N481Y substitution in its haemagglutinin cannot use receptor CD46 as efficiently as that having the haemagglutinin of the Edmonston laboratory strain. J Gen Virol 2006;87:1643–1648.
23 Tahara M, Takeda M, Yanagi Y: Contributions of matrix and large protein genes of the measles virus Edmonston strain to growth in cultured cells as revealed by recombinant viruses. J Virol 2005;79:15218–15225.
24 Tahara M, Takeda M, Yanagi Y: Altered interaction of the matrix protein with the cytoplasmic tail of hemagglutinin modulates measles virus growth by affecting virus assembly and cell-cell fusion. J Virol 2007;81: 6827–6836.
25 Pohl C, Duprex WP, Krohne G, Rima BK, Schneider-Schaulies S: Measles virus M and F proteins associate with detergent-resistant membrane fractions and promote formation of virus-like particles. J Gen Virol 2007;88: 1243–1250.
26 Nagai M, Xin JY, Yoshida N, Miyata A, Fujino M, Ihara T, Yoshikawa T, Asano Y, Nakayama T: Modified adult measles in outbreaks in Japan, 2007–2008. J Med Virol 2009;81:1094–1101.
27 Nakayama T, Komase K, Uzuka R, Hoshi A, Okafuji T: Leucine at position 278 of the AIK-C measles virus vaccine strain fusion protein is responsible for reduced syncytium formation. J Gen Virol 2001;82:2143–2150.
28 Kumada A, Komase K, Nakayama T: Recombinant measles AIK-C strain expressing current wild-type hemagglutinin protein. Vaccine 2004;22:309–316.
29 Calain P, Roux L: The rule of six, a basic feature for efficient replication of Sendai virus defective interfering RNA. J Virol 1993;67: 4822–4830.
30 Rager M, Vongpunsawad S, Duprex WP, Cattaneo R: Polyploid measles virus with hexametric genome length. EMBO J 2002;21: 2364–2372.
31 Oldstone MBA, Homann D, Lewicki H, Stevenson D: One, two, or three step: measles virus receptor dance (minireview). Virology 2002;299:162–163.
32 Tahara M, Takeda M, Seki F, Hashiguchi T, Yanagi Y: Multiple amino acid substitutions in hemagglutinin are necessary for wild-type measles virus to acquire the ability to use receptor CD46 efficiently. J Virol 2007; 81:2564–2572.
33 Masse N, Ainouze M, Neel B, Wild TF, Buckland R, Langedijk JP: Measles virus (MV) hemagglutinin: evidence that attachment sites for MV receptors SLAM and CD46 overlap on the globular head. J Virol 2004;78: 9051–9063.
34 Vongpunsawad S, Oezgun N, Braun W, Cattaneo R: Selectively receptor-blind measles viruses: identification of residues necessary for SLAM- or CD46-induced fusion and their localization on a new hemagglutinin structural model. J Virol 2004;78:302–313.
35 Hashiguchi T, Kajikawa M, Maita N, Takeda M, Kuroki K, Sasaki K, Kohda D, Yanagi Y, Maenaka K: Crystal structure of measles virus hemagglutinin provides insight into effective vaccines. Proc Natl Acad Sci USA 2007;104:19535–19540.
36 Navaratnarajah CK, Vongpunsawad S, Oezguen N, Stehle T, Braun W, Hashiguchi T, Maenaka K, Yanagi Y, Cattaneo R: Dynamic interaction of the measles virus hemagglutinin with its receptor signaling lymphocytic activation molecule (SLAM, CD150). J Biol Chem 2008;283:11763–11771.
37 Santiago C, Bjorling E, Stehle T, Casasnovas JM: Distinct kinetics for binding of the CD46 and SLAM receptors to overlapping sites in the measles virus hemagglutinin protein. J Biol Chem 2002;277:32294–32301.
38 Takeuchi K, Miyajima N, Kobune F, Tashiro M: Comparative nucleotide sequence analysis of the entire genomes of B95a cell-isolated and Vero cell-isolated viruses from the same patient. Virus Genes 2000;20:253–257.
39 Naim HY, Ehler E, Billeter MA: Measles virus matrix protein specifies apical virus release and glycoprotein sorting in epithelial cells. EMBO J 2000;19:3576–3585.
40 Runkler N, Dietzel E, Moll M, Klenk HD, Maisner A: Glycoprotein targeting signals influence the distribution of measles virus envelop proteins and virus spread in lymphocytes. J Gen Virol 2008;89:687–696.
41 Okada H, Itoh M, Nagata K, Takeuchi K: Previously unrecognized amino acid substitutions in the hemagglutinin and fusion proteins of measles virus modulate cell-cell fusion, hemadsorption, virus growth, and penetration rate. J Virol 2009;83:8713–8721.
42 Takeda M: Measles virus breaks through epithelial cell barriers to achieve transmission. J Clin Invest 2008;118:2386–2389.
43 Leonard VHJ, Sinn PL, Hodge G, Miest T, Devaux P, Oezguen N, Braun W, McCray PB Jr, McChesney MB, Cattaneo R: Measles virus blind to its epithelial cell receptor remains virulent in rhesus monkeys but cannot cross the airway epithelium and is not shed. J Clin Invest 2008;118:2448–2458.

Microbiology and Immunology

Microbiol Immunol 2011; **55**: 518–524
doi:10.1111/j.1348-0421.2011.00339.x

NOTE

Remarkable similarity in genome nucleotide sequences between the Schwarz FF-8 and AIK-C measles virus vaccine strains and apparent nucleotide differences in the phosphoprotein gene

Chie Ito[1], Shinji Ohgimoto[1], Seiichi Kato[2], Luna Bhatta Sharma[1], Minoru Ayata[1], Katsuhiro Komase[3], Kaoru Takeuchi[2], Toshiaki Ihara[4], and Hisashi Ogura[1]

[1]Department of Virology, Osaka City University Medical School, 1-4-3 Asahimachi, Abeno-ku, Osaka, Osaka 545-8585, [2]Department of Infection Biology, Institute of Basic Medical Sciences, University of Tsukuba, 1-1-1 Tennodai, Tsukuba, Ibaraki 305-8575, [3]Department of Virology 3, National Institute of Infectious Diseases, 4-7-1 Gakuen, Musashi-murayama, Tokyo 208-0011, and [4]Department of Pediatrics, National Mie Hospital, 357 Osatokubota-cho, Tsu, Mie 514-0125, Japan

ABSTRACT

The Schwarz FF-8 (FF-8) and AIK-C measles virus vaccine strains are currently used for vaccination in Japan. Here, the complete genome nucleotide sequence of the FF-8 strain has been determined and its genome sequence found to be remarkably similar to that of the AIK-C strain. These two strains are differentiated only by two nucleotide differences in the phosphoprotein gene. Since the FF-8 strain does not possess the amino acid substitutions in the phospho- and fusion proteins which are responsible for the temperature-sensitivity and small syncytium formation phenotypes of the AIK-C strain, respectively, other unidentified common mechanisms likely attenuate both the FF-8 and AIK-C strains.

Key words AIK-C, measles virus, Schwarz FF-8, vaccine.

Measles is a highly contagious disease and remains an important cause of morbidity and mortality among children in countries with a limited health infrastructure. The causative agent, MV, can be controlled effectively by immunization with live attenuated vaccines. Global measles mortality has declined dramatically through mass vaccination (1, 2), routine vaccination having substantially reduced the incidence of measles in many industrialized countries. These facts clearly illustrate the safety and effectiveness of MV vaccines. In Japan, the number of measles cases has decreased dramatically since measles vaccines were added to the routine immunization schedule in 1978 (3–6).

Three MV vaccine strains, AIK-C, FF-8, and CAM-70, are currently used for routine vaccination in Japan. The AIK-C and FF-8 strains were developed independently from the Edmonston strain of MV by serial propagation in heterologous cells and tissues, as were most other vaccine strains currently used worldwide (7–11). On the other hand, the CAM-70 strain was developed from the Tanabe strain of MV by a process similar to that used to develop the Edmonston-lineage vaccine strains (10, 12, 13). The safety and effectiveness of the three vaccine strains are well established, and are similar to that of other internationally available measles vaccines (7, 11, 14, 15). However, the molecular mechanism of their

Correspondence
Shinji Ohgimoto, Department of Virology, Osaka City University Medical School, 1-4-3 Asahimachi, Abeno-ku, Osaka 545-8585, Japan.
Tel: +81 6 6645 3911; fax: +81 6 6645 3912; email: ohgimoto@med.osaka-cu.ac.jp

Received 13 December 2010; revised 24 February 2011; accepted 8 March 2011.

List of Abbreviations: a.a., amino acid; CEF, chicken embryonic fibroblasts; FF-8, Schwarz FF-8; F protein, fusion protein; H protein, hemagglutinin protein; IFN, interferon; L protein, large protein; MOI, multiplicity·of infection; M protein, matrix protein; MOI, multiplicity of infection; MV, measles virus; N protein, nucleocapsid protein; nt, nucleotide; P protein, phosphoprotein; RNP complex, ribonucleoprotein complex; SLAM, signaling lymphocyte activation molecule; $TCID_{50}$, median tissue culture infective dose; *ts*, temperature-sensitive

attenuation is not well understood and remains a subject of investigation.

Measles virus, an enveloped virus with a non-segmented negative-strand RNA genome, belongs to the genus *Morbilivirus* in the family *Paramyxoviridae*. The MV genome of 15,894 nucleotides consists of six tandem-linked genes that encode the N, P, M, F, H, and L proteins. The P gene, in addition to the P protein, encodes two accessory proteins, the C and V proteins. The C protein is synthesized by an alternative translational initiation in a different reading frame, and the V protein is translated from the mRNA edited by a cotranscriptional insertion of a single non-templated G residue. The N protein encapsidates the viral genomic RNA, the N protein-encapsidated viral genome being associated with a viral RNA-dependent RNA polymerase composed of the P and L proteins, forming a helical RNP complex. In infected cells, the viral RNA-dependent RNA polymerase both transcribes the genomic RNA into mRNAs and replicates the viral genome (11). The C and V proteins promote viral replication by antagonizing host IFN responses (16–29). In addition, the C protein modulates viral mRNA transcription and genome replication (30), this modulation presumably being a mechanism for the C protein to inhibit IFN induction (21, 22). The H and F proteins are integral membrane glycoproteins that mediate cell surface recognition, membrane fusion, and virus entry. The M protein interacts with the RNP complex and the cytoplasmic tails of the H and F proteins, and plays an important role in assembly and budding of the viral particles (11).

The genome nucleotide sequences of the AIK-C and CAM-70 strains have already been analyzed (31–33), and molecular characterization of these vaccine strains has been proceeding. The AIK-C strain has long been known to exhibit a *ts* phenotype, plaque formation of the AIK-C strain in cultured cells dramatically decreasing at temperatures of 39°C and higher (34). Molecular analysis has revealed that the *ts* phenotype of the AIK-C strain results from reduced RNA polymerase activity at high temperatures, this being caused by the amino acid substitution L439P in the P protein (35). The *ts* phenotype may explain the underlying molecular mechanism causing attenuation of the AIK-C strain. In addition, reduced ability of the CAM-70 H protein to use cellular receptors CD46 and the signaling lymphocyte activation molecule (SLAM, also called CD150) has been proposed as a possible mechanism of attenuation of the CAM-70 strain (36). However, the complete genome nucleotide sequence of the FF-8 strain has not yet been reported and little is known at the molecular level about this strain. In the present study we therefore determined the complete genome nucleotide sequence of the FF-8 strain.

We infected B95a cells with a commercially available vaccine vial of the FF-8 strain (Takeda Pharmaceutical, Osaka, Japan) at a MOI of 0.005 $TCID_{50}$/cell, and harvested the infected cells 2 days post infection. We then isolated total RNA from the infected cells using an RNeasy mini kit (Qiagen, Hilden, Germany) and reverse-transcribed it into cDNA using each of the specific sense primers for the MV genes and the Superscript III first-strand synthesis system for RT-PCR (Invitrogen, Carlsbad, CA, USA). We amplified the cDNA by PCR using Platinum Pfx DNA polymerase (Invitrogen) with each set of MV-specific sense and antisense primers. cDNAs of the leader and trailer regions were amplified using the 5′ RACE system for rapid amplification of cDNA ends version 2.0 (Invitrogen) and MV-specific primers. We cloned the amplified PCR product into a pCR-Blunt-II-TOPO vector (Invitrogen), and sequenced three clones of the cDNA using the Big Dye terminator cycle sequencing kit and an ABI 3130 Genetic Analyzer (Applied Biosystems, Foster City, CA, USA). To further confirm the sequence, we repeated the procedure described above using another vaccine vial of the FF-8 strain.

The complete genome nucleotide sequence of the FF-8 strain has been deposited in the DNA Data Bank of Japan/European Molecular Biology Laboratory/GenBank with accession number AB591381. Comparison of the nt sequence of the FF-8 N gene with those of the Edmonston-lineage MV vaccine strains revealed that the FF-8 strain is genetically very close to the AIK-C vaccine strain (31). We then compared the genome nt sequence of the FF-8 strain with the two most recently reported complete genome sequences of the AIK-C strain (GenBank accession numbers AF266286 and AB046218) and found nt differences among them at 16 nt positions (Table 1). Since there are nt differences between the two reported AIK-C sequences at 14 positions, we propagated a commercially available vaccine vial of the AIK-C strain (Kitasato Institute Research Center for Biologicals, Saitama, Japan) in B95a cells and newly determined its nucleotide sequence in the regions encompassing the 16 nt positions. The nucleotides of our AIK-C sequence were identical to those of the FF-8 strain at all positions except nt positions 1959 and 3122, and also identical to one or both of the reported AIK-C sequences at all positions (Table 1). Nakayama *et al.* have previously reported that the AIK-C strain is a mixture of at least two types of virus (37). The differences among reported AIK-C sequences may reflect variations in the genome sequences of viruses in AIK-C virus stocks. Similarly, there should also be genome sequence variations in FF-8 virus stocks, and the genome sequences of the FF-8 viruses should consist of the sequence described above and its variations. We concluded that the genome nucleotide sequences of the

Table 1. Nucleotide differences in the genome between the FF-8 and AIK-C MV vaccine strains

Region	Nucleotide position	Strain†				
		Schwarz FF-8	AIK-C (AF266286)	AIK-C (AB046218)	AIK-C‡ (S58435)	AIK-C§ (this study)
N noncoding	1716	C	C	T	C	C
P coding	**1959¶**	**A**	**G**	**G**	**G**	**G**
P coding	**3122¶**	**T**	**C**	**C**	**C**	**C**
M coding	3506	C	G	C	C	C
F noncoding	5030	C	T	C	C	C
F coding	6291	C	C	A	A	C
F coding	6712	C	A	C	C	C
L coding	10344	A	A	T	A	A
L coding	10857	A	A	G	A	A
L coding	11158	A	A	G	A	A
L coding	11711	A	A	G	A	A
L coding	12671	G	G	A	G	G
L coding	14339	G	G	A	G	G
L coding	14651	G	G	A	G	G
L coding	15454	A	G	A	G	A
L coding	15622	T	T	C	T	T

†Comparison of genome sequence of the FF-8 strain with two reported sequences of the AIK-C strain (Accession numbers AF266286 and AB046218).
‡Nucleotides of another reported AIK-C sequence (Accession number S58435) at the 16 nucleotide positions.
§Newly determined nucleotide sequences of the genome regions encompassing the 16 nucleotide positions of a vaccine vial-derived AIK-C strain.
¶Bold face entries represent the positions where the nucleotide of the FF-8 strain is consistently different from that of the AIK-C sequences.

FF-8 strain are remarkably similar to those of the AIK-C strain. The nucleotide differences at positions 1959 and 3122 in the P gene appear to differentiate the two vaccine strains (Table 1).

The FF-8 and AIK-C strains are propagated in CEF to produce live attenuated MV vaccines. In this study, we propagated vaccine vials of the FF-8 and AIK-C strains in B95a cells once only, and determined the nucleotide sequence of the propagated viruses. Then, we compared our FF-8 and AIK-C genome sequences with the reported sequences of the AIK-C strain propagated in CEF (GenBank accession numbers AB046218 and S58435) (35, 38). The nts of our FF-8 and AIK-C sequences were identical to one or both of the nts of the reported AIK-C sequences (AB046218 and S58435) at all nt positions except nt positions 1959, 3122, and 6291 for the FF-8 sequence and nt position 6291 for the AIK-C sequence. The AIK-C virus stock propagated in CEF also contained viruses possessing the nt C at position 6291, which is identical to the nt of our FF-8 and AIK-C sequences (37). Thus, our FF-8 and AIK-C sequences are unlikely to be far from the nt sequences of the viruses in each of the vaccine vials, although minimal nt changes due to propagation in B95a cells could not be excluded.

The FF-8 strain has been reported to be a descendant of another MV vaccine strain, Schwarz (7). Genome nucleotide comparison among Edmonston-lineage vaccine strains has revealed that the AIK-C strain is genetically distant from the Schwarz strain (31). However, our results indicate that the FF-8 strain is genetically very close to the AIK-C strain and that the FF-8 strain may not be a descendant of the Schwarz strain.

The nt difference at position 1959 in the P gene results in an a.a. difference at a.a. position 44 in the C protein, a glutamic acid for the FF-8 strain, and a glycine for the AIK-C strain (Table 2), but this is not the case for the P

Table 2. Nucleotide differences in the P gene and the resulting amino acid differences in P gene products between the FF-8 and AIK-C MV vaccine strains

Nucleotide position	Nucleotide difference FF-8 – AIK-C	Protein	Amino acid position	Amino acid difference FF-8 – AIK-C
1959†	A–G	C	44	E–G
3122	T–C	P	439	L–P

†The nucleotide difference at nt position 1959 does not result in an amino acid difference in the P and V proteins.

and V proteins. We further compared the a.a. sequences of the C proteins among the Edmonston lineage vaccine strains, and found that the glutamic acid at a.a. position 44 is unique to the FF-8 C protein, and that the glycine is common among the other Edmonston-lineage vaccine strains (31). The MV C protein antagonizes host cell IFN responses (18, 20–22, 26), C-deficient recombinant MVs being unable to grow efficiently in cultured cells possessing a functional IFN system (21, 22, 28, 39). In addition, C protein modulates viral mRNA transcription and genome replication (30). We therefore decided to examine whether the a.a. substitution G44E in the FF-8 C protein affects virus growth in cells with a functional IFN system. For this purpose, we used a cloned MV IC323 that can be rescued from the full-length genomic cDNA of the wild-type IC-B strain (40). We replaced the P gene of IC323 with the one derived from the FF-8 strain, and successfully rescued IC323 possessing the FF-8 P gene, designated IC-FF-8 P (Fig. 1a). We also generated a recombinant MV IC-FF-8 P-C_{E44G} whose P gene encodes FF-8 P and V proteins as well as AIK-C C protein (Fig. 1a). We then examined virus growth of the recombinant MVs in HeLa and 293 cells expressing human SLAM (HeLa/SLAM and 293/SLAM, respectively) with their IFN systems intact (21, 28, 39). In

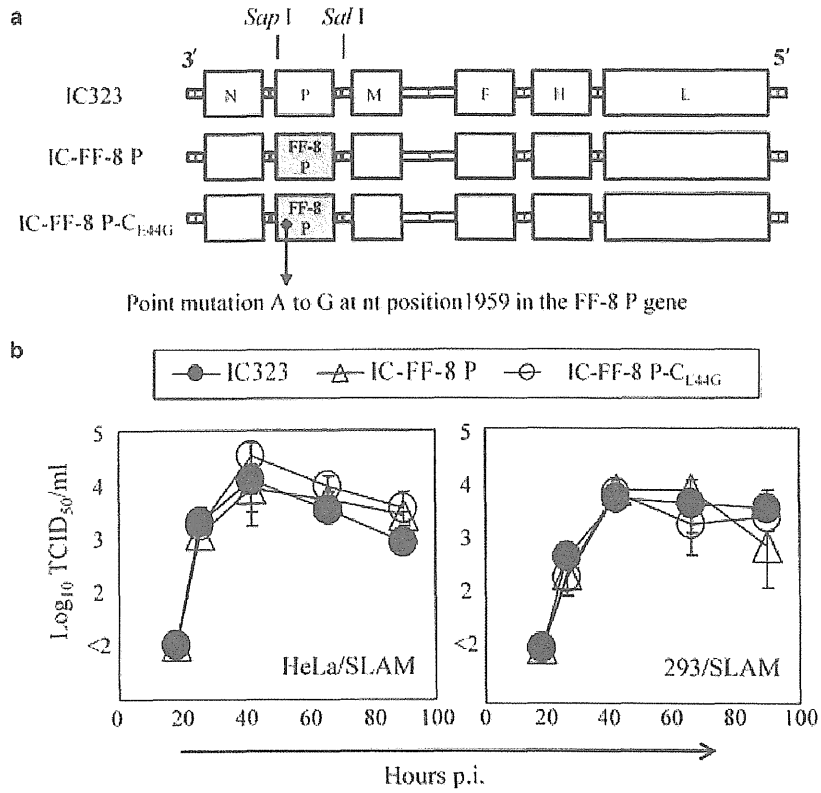

Fig. 1. Growth kinetics of recombinant MVs in cell lines possessing functional IFN systems. (a) Schematic diagram of the recombinant MVs. Wide boxes indicate open reading frames of the MV N, P, M, F, H, and L proteins. Narrow boxes indicate untranslated regions, and vertical lines in the untranslated regions indicate intergenic trinucleotides. Narrow boxes at the 3′ and 5′ genome termini are leader and trailer sequences. Regions derived from the FF-8 vaccine strain are shaded, and regions from IC323 are in white. Restriction enzyme sites used to replace the P gene of IC323 with the corresponding region of the FF-8 strain are indicated. IC-FF-8 P-C_{E44G} possesses a point mutation A to G at nt position 1959 in the FF-8 P gene and its P gene encodes the FF-8 P and V proteins and the AIK-C C protein. (b) Growth kinetics of recombinant MVs, IC323, IC-FF8 P, and IC-FF-8 P-C_{E44G} in HeLa/SLAM and 293/SLAM at 37°C. To generate HeLa/SLAM and 293/SLAM, HeLa and 293 cells were infected with retroviruses expressing the neomycin-resistance gene and human SLAM, and the transduced cells were cultured in the presence of 1mg/mL of G418 (Geneticin; Nacalai Tesque, Tokyo, Japan). Expression of human SLAM on HeLa/SLAM and 293/SLAM was confirmed by immunofluorescent staining with phycoerythrin-conjugated anti-SLAM monoclonal antibody (clone A12) or PE-conjugated mouse IgG_1 isotype-control antibody (BD Biosciences, San Jose, CA, USA) for flow cytometric analysis on a FACS Calibur (BD Biosciences) (data not shown). HeLa/SLAM or 293/SLAM was infected with each of the recombinant MVs at an MOI of 0.01 $TCID_{50}$/cell. Infected culture medium and cells were harvested together at the indicated time points. After freezing and thawing, infectivity titers were determined by measuring the $TCID_{50}$ in B95a cells. The means ± standard deviations from three independent experiments are shown. p.i., post-infection.

both HeLa/SLAM and 293/SLAM, IC-FF-8 P and IC-FF-8 P-C_{E44G} grew as efficiently as IC323 (Fig. 1b), a result consistent with a previous report that the C protein of another MV vaccine strain Ed-tag is fully functional (39). Thus, both FF-8 and AIK-C C proteins appear to be intact in regard to antagonizing the IFN response, and do not attenuate viral transcription and replication.

The nucleotide difference at position 3122 in the P gene results in an a.a. difference at a.a. position 439 in P protein, a leucine for the FF-8 strain, and a proline for the AIK-C strain (Table 2). When further compared with the P proteins of the other Edmonston lineage vaccine strains, the proline at a.a. position 439 appears to be unique to the AIK-C P protein, whereas the leucine at this position is common among the other MV vaccine P proteins (31). The AIK-C strain is known to exhibit a *ts* phenotype, plaque formation of the AIK-C strain in cultured cells dramatically decreasing at temperatures of 39°C and higher (34). The *ts* phenotype of the AIK-C strain results from reduced RNA polymerase activity at higher temperatures, this being attributed to the a.a. substitution L439P in the P protein (35). On the contrary, consistent with the a.a. sequence of FF-8 P protein which lacks the substitution L439P (Table 2), the FF-8 strain does not exhibit the *ts* phenotype (34).

The AIK-C strain contains a type of virus with a leucine instead of a phenylalanine at a.a. position 278 in the F protein, a substitution which results from the nt change C to A at nt position 6291 in the F gene (Table 1) (37). This type of virus induces small syncytia in cultured cells (37). In the present study, we sequenced six clones of the PCR products generated from the FF-8 genomes and did not find a clone with the nt A at nt position 6291. Thus, the FF-8 strain is unlikely to contain the type of virus with a leucine at a.a. position 278 in the F protein.

We then examined whether the differences between the AIK-C and FF-8 strains described above affect viral growth in cultured cells. We included a wild-type MV IC323 for comparison. While the FF-8 strain grew as efficiently as IC323 in all cell types of B95a cells, Vero cells expressing human SLAM (Vero/SLAM), and HeLa/SLAM, growth of the AIK-C strain was slightly slower than that of the other two (Fig. 2). The slower growth of the AIK-C strain may result from the *ts* phenotype and/or the presence of the small syncytium-inducing viruses.

It has been proposed that attenuation of the AIK-C strain is caused by the *ts* phenotype and the presence of small syncytium-inducing viruses (35, 37). As described above, the genome nt sequences of the FF-8 strain are remarkably similar to those of the AIK-C strain. The a.a. substitution G44E, which is unique to the FF-8 C protein, does not affect viral growth in IFN system-intact cells and does not appear to contribute to attenuation of

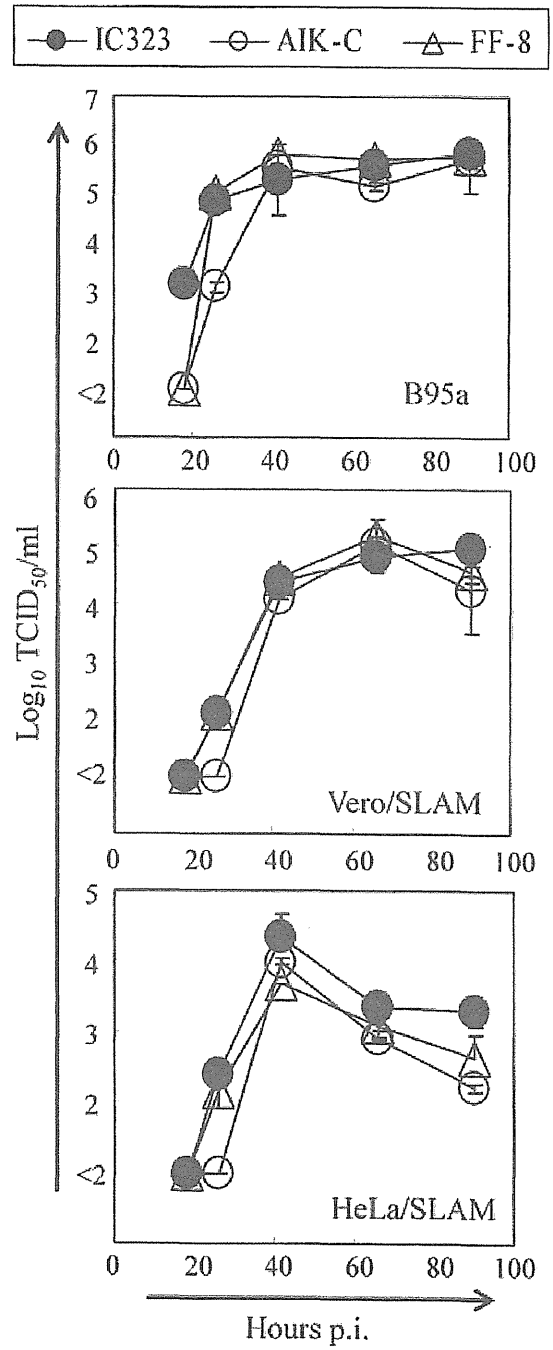

Fig. 2. Growth kinetics of MV strains in cultured cells at 37°C. B95a cells, Vero/SLAM, or HeLa/SLAM were infected with each of the MV strains at an MOI of 0.01 $TCID_{50}$/cell. Infected culture medium and cells were harvested together at the indicated time points. After freezing and thawing, infectivity titers were determined by measuring the $TCID_{50}$ in B95a cells. The means±standard deviations from three independent experiments are shown. p.i., post-infection.

the FF-8 strain. Moreover, the FF-8 strain does not exhibit the *ts* phenotype (34) and is unlikely to contain the small syncytium-inducing type of virus. Nonetheless, the FF-8 strain is attenuated enough to be safe for use in routine vaccination. These facts suggest that the phenotypes unique to the AIK-C strain may not be the major mechanism of AIK-C attenuation, and that there are other common mechanisms that attenuate both the FF-8 and AIK-C strains, and maybe other MV vaccine strains. The unique phenotypes of the AIK-C strain may rather contribute to further attenuation of the virus.

A previous clinical evaluation has revealed remarkable similarity between the AIK-C and FF-8 strains in immunogenicity and reactogenicity (7). However, in view of the identity and differences in their genome sequences between the FF-8 and AIK-C strains, reevaluation and precise comparison of efficacy and adverse reactions caused by vaccination with the FF-8 and AIK-C strains would help to clarify the significance of the a.a. substitutions that are specific to the AIK-C strain.

ACKNOWLEDGMENTS

We thank M. Takeda and Y. Yanagi for providing pCAG-IC-N, pCAG-IC-PΔC, and pGEM-9301-L, and R. Tanaka for excellent technical assistance. We also thank the staff at the Central Laboratory of Osaka City University Medical School for their technical support.

This work was supported by a grant from the Osaka Foundation for Incurable Diseases.

REFERENCES

1. Centers for Disease Control and Prevention. (2009) Global measles mortality, 2000–2008. *MMWR* **58:** 1321–6.
2. Wolfson L.J., Strebel P.M., Gacic-Dobo M., Hoekstra E.J., McFarland J.W., Hersh B.S. (2005) Measles Initiative. Has the 2005 measles mortality reduction goal been achieved? A natural history modelling study. *Lancet* **369:** 191–200.
3. Centers for Disease Control and Prevention. (2008) Progress toward measles elimination – Japan, 1999–2008. *MMWR* **57:** 1049–52.
4. Centers for Disease Control and Prevention. (2009) Progress toward the 2012 measles elimination goal – Western pacific region, 1990–2008. *MMWR* **58:** 669–73.
5. Morita Y., Suzuki T., Shiono M., Shiobara M., Saitoh M., Tsukagoshi H., Yoshizumi M., Ishioka T., Kato M., Kozawa K., Tanaka-Taya K., Yasui Y., Noda M., Okabe N., Kimura H. (2007) Sequence and phylogenetic analysis of the nucleoprotein (N) gene in measles viruses prevalent in Gunma, Japan, in 2007. *Jpn J Infect Dis* **60:** 402–4.
6. Okafuji T., Okafuji T., Fujino M., Nakayama T. 2006. Current status of measles in Japan: molecular and seroepidemiological studies. *J Infect Chemother* **12:** 343–8.
7. Hirayama M. (1983) Measles vaccines used in Japan. *Rev Infect Dis* **5:** 495–503.
8. Makino S. (1977) Measles virus mutants and their implication in basic and applied virology. *Ann Microbiol (Inst Pasteur)* **128B:** 507–15.
9. Makino S. (1983) Development and characteristics of live AIK-C measles virus vaccine: a brief report. *Rev Infect Dis* **5:** 504–5.
10. Ueda S. (2009) Development of measles vaccines in Japan. *Vaccine* **27:** 3230–1.
11. Griffin D.E. (2007) Measles virus. In:Knipe D.M., Howley P.M., Griffin D.E., Lamb R.A., Martin M.A., Roizman B., Straus S.E., eds. *Fields Virology*, 5th ed., Philadelphia, PA: Lippincott Williams & Wilkins, pp. 1551–85.
12. Ueda S., Takahashi M., Minekawa Y., Ogino T., Suzuki N., Yamanishi K., Baba K., Okuno Y. (1970a) Studies on further attenuated live measles vaccine. Part I. Adaptation of measles virus to the chorioallantoic membrane of chick embryo and clinical tests on the strain. *Biken J* **13:** 111–6.
13. Ueda S., Takahashi M., Minekawa Y., Ogino T., Suzuki N., Yamanishi K., Baba K., Okuno Y. (1970b) Studies on further attenuated live measles vaccine. Part II. Correlation between the titer of the vaccine, the antibody response and clinical reactions. *Biken J* **13:** 117–20.
14. Okuno Y., Ueda S., Kurimura T., Suzuki N., Yamanishi K., Baba K., Takahashi M. (1971) Studies on further attenuated live measles vaccine. Part VII. Development and evaluation of CAM-70 measles virus vaccine. *Biken J* **14:** 253–8.
15. Ozaki T., Matsui Y, Kajita Y., Nishimura N. (2002) Clinical and serological studies on CAM-70 live attenuated measles vaccine: an 18-year survey at a pediatric clinic in Japan. *Vaccine* **20:** 2618–22.
16. Caignard G., Guerbois M., Labernardiere J.L., Jacob Y., Jones L.M., Wild F., Tangy F., Vidalain P.O. (2007) Measles virus V protein blocks Jak1-mediated phosphorylation of STAT1 to escape IFN-alpha/beta signaling. *Virology* **368:** 351–62.
17. Devaux P., Cattaneo, R. (2004) Measles virus phosphoprotein gene products: conformational flexibility of the P/V protein amino-terminal domain and C protein infectivity factor function. *J. Virol.* **78:** 11,632–40.
18. Fontana J.M., Bankamp B., Bellini W.J., Rota P.A. (2008) Regulation of interferon signaling by the C and V proteins from attenuated and wild-type strains of measles virus. *Virology* **374:** 71–81.
19. Ikegame S., Takeda M., Ohno S., Nakatsu Y., Nakanishi Y., Yanagi Y. (2010) Both RIG-I and MDA5 RNA helicases contribute to the induction of alpha/beta interferon in measles virus-infected human cells. *J Virol* **84:** 372–9.
20. McAllister C.S., Toth A.M., Zhang P., Devaux P., Cattaneo R., Samuel C.E. (2010) Mechanisms of protein kinase PKR-mediated amplification of beta interferon induction by C protein-deficient measles virus. *J Virol* **84:** 380–6.
21. Nakatsu Y., Takeda M., Ohno S., Koga R., Yanagi Y. (2006) Translational inhibition and increased interferon induction in cells infected with C protein-deficient measles virus. *J Virol* **80:** 11,861–7.
22. Nakatsu Y., Takeda M., Ohno S., Shirogane Y., Iwasaki M., Yanagi Y. (2008) Measles virus circumvents the host interferon response by different actions of the C and V proteins. *J Virol* **82:** 8296–306.
23. Ohno S., Ono N., Takeda M., Takeuchi K., Yanagi Y. (2004) Dissection of measles virus V protein in relation to its ability to block alpha/beta interferon signal transduction. *J Gen Virol* **85:** 2991–9.
24. Palosaari H., Parisien J.P., Rodriguez J.J., Ulane C.M., Horvath C.M. (2003) STAT protein interference and suppression of cytokine signal transduction by measles virus V protein. *J Virol* **77:** 7635–44.
25. Pfaller C.K., Conzelmann K.K. (2008) Measles virus V protein is a decoy substrate for IκB kinase alpha and prevents Toll-like receptor 7/9-mediated interferon induction. *J Virol* **82:** 12,365–73.

26. Shaffer J.A., Bellini W.J., Rota P.A. (2003) The C protein of measles virus inhibits the type I interferon response. *Virology* **315:** 389–97.
27. Takeuchi K., Kadota S.I., Takeda M., Miyajima N., Nagata K. (2003) Measles virus V protein blocks interferon (IFN)-alpha/beta but not IFN-gamma signaling by inhibiting STAT1 and STAT2 phosphorylation. *FEBS Lett* **545:** 177–82.
28. Takeuchi K., Takeda M., Miyajima N., Ami Y., Nagata N., Suzaki Y., Shahnewaz J., Kadota S., Nagata K. (2005) Stringent requirement for the C protein of wild-type measles virus for growth both *in vitro* and in macaques. *J Virol* **79:** 7838–44.
29. Yokota S., Sato H., Kubota T., Yokosawa N., Amano K., Fujii N. (2003) Measles virus suppresses interferon-alpha signaling pathway: suppression of Jak1 phosphorylation and association of viral accessory proteins, C and V, with interferon-alpha receptor complex. *Virology* **306:** 135–46.
30. Reutter G.L., Cortese-Grogan C., Wilson J., Moyer S.A. (2001) Mutations in the measles virus C protein that up regulate viral RNA synthesis. *Virology* **285:** 100–9.
31. Parks C.L., Lerch R.A., Walpita P., Wang H.P., Sidhu M.S., Udem S.A. (2001) Comparison of predicted amino acid sequences of measles virus strains in the Edmonston vaccine lineage. *J Virol* **75:** 910–20.
32. Parks C.L., Lerch R.A., Walpita P., Wang H.P., Sidhu M.S., Udem S.A. (2001) Analysis of the noncoding regions of measles virus strains in the Edmonston vaccine lineage. *J Virol* **75:** 921–33.
33. Borges M.B., Caride E., Jabor A.V., Malachias J.M., Freire M.S., Homma A., Galler R. (2008) Study of the genetic stability of measles virus CAM-70 vaccine strain after serial passages in chicken embryo fibroblasts primary cultures. *Virus Genes* **36:** 35–44.
34. Fukuda A., Sugiura A. (1983) Temperature-dependent growth restriction in measles vaccine strains. *Jpn J Med Sci Biol* **36:** 331–5.
35. Komase K., Nakayama T., Iijima M., Miki K., Kawanishi R., Uejima H. (2006) The phosphoprotein of attenuated measles AIK-C vaccine strain contributes to its temperature-sensitive phenotype. *Vaccine* **24:** 826–34.
36. Kato S., Ohgimoto S., Sharma L.B., Kurazono S., Ayata M., Komase K., Takeda M., Takeuchi K., Ihara T., Ogura H. (2009) Reduced ability of hemagglutinin of the CAM-70 measles virus vaccine strain to use receptors CD46 and SLAM. *Vaccine* **27:** 3838–48.
37. Nakayama T., Komase M., Uzuka R., Hoshi A., Okafuji T. (2001) Leucine at position 278 of the AIK-C measles virus vaccine strain fusion protein is responsible for reduced syncytium formation. *J Gen Virol* **82:** 2143–50.
38. Mori T., Sakai K., Hashimoto H., Makino S. (1993) Molecular cloning and complete nucleotide sequence of the genomic RNA of the AIK-C strain of attenuated measles virus. *Virus Genes* **7:** 67–81.
39. Nakatsu Y., Takeda M., Iwasaki M., Yanagi Y. (2009) A highly attenuated measles virus vaccine strain encodes a fully functional C protein. *J Virol* **83:**11,996–2001.
40. Takeda M., Takeuchi K., Miyajima N., Kobune F., Ami Y., Nagata N., Suzaki Y., Nagai Y., Tashiro M. (2000) Recovery of pathogenic measles virus from cloned cDNA. *J Virol* **74:** 6643–47.

nature
structural &
molecular biology

Structure of the measles virus hemagglutinin bound to its cellular receptor SLAM

Takao Hashiguchi[1], Toyoyuki Ose[2], Marie Kubota[1], Nobuo Maita[3,4], Jun Kamishikiryo[3], Katsumi Maenaka[2,3,5] & Yusuke Yanagi[1]

Measles virus, a major cause of childhood morbidity and mortality worldwide, predominantly infects immune cells using signaling lymphocyte activation molecule (SLAM) as a cellular receptor. Here we present crystal structures of measles virus hemagglutinin (MV-H), the receptor-binding glycoprotein, in complex with SLAM. The MV-H head domain binds to a β-sheet of the membrane-distal ectodomain of SLAM using the side of its β-propeller fold. This is distinct from attachment proteins of other paramyxoviruses that bind receptors using the top of their β-propeller. The structure provides templates for antiviral drug design, an explanation for the effectiveness of the measles virus vaccine, and a model of the homophilic SLAM-SLAM interaction involved in immune modulations. Notably, the crystal structures obtained show two forms of the MV-H–SLAM tetrameric assembly (dimer of dimers), which may have implications for the mechanism of fusion triggering.

Measles still causes 4% of all deaths in children under age 5 worldwide, despite the availability of an effective live vaccine and the great efforts made to deliver vaccine to children throughout the world[1,2]. Outbreaks continue to occur, even in industrialized nations when vaccination coverage is low[2]. Measles virus is an enveloped virus with a nonsegmented, negative-strand RNA genome, and is classified as a member of the family Paramyxoviridae[3]. To enter a cell, enveloped viruses must bind to their receptors on host cells and induce fusion of the viral membrane with the host cell membrane[4]. Paramyxoviruses attach to and fuse with host membranes at the cell surface, using two distinct envelope proteins. Of these, the attachment protein is responsible for receptor binding whereas the fusion protein mediates membrane fusion[5]. The mechanism by which receptor binding leads to fusion is not well understood[5–8]. The attachment protein could undergo a conformational change upon binding to receptor. This conformational change would destabilize the metastable fusion protein, causing its refolding, which in turn would drive membrane fusion. Alternatively, the attachment protein could serve as a clamp that stabilizes the fusion protein in its prefusion state. Receptor binding of the attachment protein would release the fusion protein from the clamp to facilitate its spontaneous conformational change. Different paramyxoviruses may use different mechanisms of fusion triggering[6–8].

Most paramyxoviruses use sialic acid–containing cell surface molecules as receptors[5]. By contrast, measles virus uses a protein molecule, SLAM (also called CD150), as a receptor[9,10]. SLAM is the prototype member of the SLAM family of receptors, which mediates important regulatory signals in immune cells and includes 2B4, CD48, CD84, CD229, CD319 and natural killer, T- and B-cell antigen (NTB-A)[11,12]. The SLAM family shares a similar immunoglobulin (Ig) domain–containing structural organization. SLAM is expressed on thymocytes, activated lymphocytes, mature dendritic cells, macrophages and platelets[12], and is also a marker for the most primitive hematopoietic stem cells[13]. It acts as a self ligand, interacting with another SLAM molecule present on an adjacent cell at a low affinity ($K_d \cong 200$ μM)[14]. The distribution and function of SLAM may explain the tropism and immunosuppressive nature of measles virus[10].

Although SLAM is the predominant receptor for wild-type, circulating field isolates of measles virus, vaccine strains of the virus use CD46 as an alternate receptor, owing to amino acid changes in the attachment protein MV-H[10,15–17]. An as-yet-unknown receptor molecule also exists on polarized epithelial cells, which may facilitate transmission via aerosol droplets[18–20].

We and others have determined the crystal structure of the receptor-binding head domain of MV-H[21,22]. The structure of the MV-H–CD46 complex has also been reported recently[23]. The MV-H head domain forms a disulfide-linked homodimer and exhibits a six-bladed β-propeller fold. Here we present the crystal structure of the MV-H head domain in complex with the critical Ig domain of marmoset (*Saguinus oedipus*) SLAM at a resolution of 3.15 Å. The structure provides the molecular basis for the effectiveness of the current measles virus vaccine and a framework for structure-based antiviral drug design. Furthermore, it sheds light on how binding of MV-H to SLAM triggers the conformational change of the measles virus fusion protein (MV-F) required for membrane fusion.

[1]Department of Virology, Faculty of Medicine, Kyushu University, Fukuoka, Japan. [2]Laboratory of Biomolecular Science, Faculty of Pharmaceutical Sciences, Hokkaido University, Sapporo, Japan. [3]Research Center for Prevention of Infectious Diseases, Medical Institute of Bioregulation, Kyushu University, Fukuoka, Japan. [4]Institute for Enzyme Research, University of Tokushima, Tokushima, Japan. [5]Core Research for Evolutional Science and Technology, Japan Science and Technology Agency, Saitama, Japan. Correspondence should be addressed to Y.Y. (yyanagi@virology.med.kyushu-u.ac.jp) or K.M. (kmaenaka-umin@umin.net).

Received 10 May 2010; accepted 29 October 2010; published online 9 January 2011; doi:10.1038/nsmb.1969

RESULTS

Crystallization of the MV-H–SLAM complex

MV-H is a type II membrane protein comprised of an N-terminal cytoplasmic tail, a transmembrane region, a stalk and a C-terminal receptor-binding head domain[3,5]. Its receptor, SLAM, is a type I membrane protein that contains an extracellular region with two Ig-like domains (V-set and C2-set) in addition to a transmembrane region and a cytoplasmic tail[11]. Of these, the membrane-distal V-set Ig domain is sufficient for receptor function[24]. SLAM from both human and marmoset species acts as a receptor for measles virus[9].

The V-set Ig domains of the human and marmoset SLAM (hSLAM-V and maSLAM-V, respectively) and the MV-H head domain were produced as described[21,25], and used for crystallization (**Table 1**). A 1:1 complex of MV-H head (residues 149–617) and maSLAM-V crystallize and diffract to a resolution of 4.5 Å. The mixture of MV-H and hSLAM-V did not crystallize. We improved diffractions by engineering a fusion construct in which the MV-H head domain (residues 184–607) and maSLAM-V (residues 30–140 with N102H and R108Y substitutions) were connected via a 12-residue flexible linker, $(Gly\text{-}Gly\text{-}Gly\text{-}Ser)_3$. We introduced the two substitutions in maSLAM-V (N102H and R108Y) to remove residues that were probably detrimental to crystal packing, on the basis of preliminary crystallization studies. The MV-H–maSLAM-V protein was expressed as a single chain, purified and methylated. Crystals diffracted to a resolution of 3.55 Å. An additional substitution, L482R, in MV-H further improved the diffraction to a resolution of 3.15 Å. We determined the structure of the MV-H–maSLAM-V complex by molecular replacement using an uncomplexed MV-H head domain (free MV-H)[21] as a search model. The bound SLAM was manually fitted into the residual electron density using the structure of CD48 as a model[26].

Overall structure of the MV-H–SLAM complex

The asymmetric unit contains two essentially identical dimers of the 1:1 MV-H–maSLAM-V complex (**Fig. 1a–c**). Wild-type MV-H has a six-bladed β-propeller fold and dimerizes using an intermolecular Cys154-Cys154 disulfide bond. Although the MV-H used for crystallization here does not contain Cys154, the homodimer is still formed by noncovalent interactions at the interface. Furthermore, the structure of complexed MV-H is essentially identical to that of free MV-H (r.m.s. deviation of 1.84 Å; 407 Cα atoms); **Fig. 1d**). Hence, no large structural change of the MV-H head domain or of its dimeric orientation occurs upon receptor binding.

The bound maSLAM-V exhibits a typical Ig-fold structure comprising the BED and AGFCC′C″ β-sheets, with a Cys32-Cys132 disulfide bond stabilizing the A-G interstrand interaction (**Fig. 1a** and **Supplementary Fig. 1a**). Previous mutational studies and the crystal structure of the free MV-H have suggested that SLAM may bind a small 'acidic patch' on the β5 sheet of MV-H[21,22,27,28]. The crystal structure of the complex presented here shows that although the β5 sheet forms the center of the SLAM-binding site, the complete binding site is assembled by the β4, β5 and β6 sheets at the side of the MV-H β-propeller. This site is bound by the AGFCC′C″ β-sheet of maSLAM-V (**Fig. 1a,c** and **Supplementary Fig. 1b**). The complex formed by individually expressed MV-H and maSLAM-V is essentially identical to that formed by the MV-H–maSLAM-V fusion protein, indicating that the single-chain construction does not substantially affect the structure of the complex (**Supplementary Fig. 1c,d**). The subsequent C2-set Ig domain of maSLAM, which was not included in our construct, can be placed continuously from the N-terminal V-set Ig domain without any steric hindrance from the bound MV-H (**Fig. 1a**), suggesting that the C2-set Ig domain is outside the MV-H-binding interface, and thus does not contribute to MV-H binding, consistent with previous domain-swapping studies[24].

Notably, the highly tilted orientation of the monomers in the MV-H homodimer[21] suggests that the SLAM-binding interface on MV-H is located far from the viral envelope (**Fig. 1a,b**). Furthermore, the mode of receptor binding by MV-H is distinct from modes of receptor binding of other paramyxovirus attachment proteins and the influenza virus neuraminidase (Flu-NA), which share the six-bladed β-propeller fold (**Fig. 1c** and **Supplementary Fig. 2**). For example, the hemagglutinin-neuraminidase of parainfluenza virus 5 (PIV5-HN), the G protein of Nipah virus (NiV-G) and Flu-NA use the top of the β-propeller for binding to their receptor or ligand[29–33]. Of these, PIV5-HN and Flu-NA use a shallow pocket at the top to bind sialic acid, whereas NiV-G uses a wide surface area at the top to bind its receptor, ephrin B2 or ephrin B3, with a small pocket into which Phe120 of ephrin B2 or Tyr120 of ephrin B3 penetrates[30,31]. MV-H is unique in its use of the side of the β-propeller fold to bind its receptor SLAM.

Table 1 Data collection and refinement statistics

	Native	MV-H–SLAM N102H R108Y fusion	MV-H L482R–SLAM N102H R108Y fusion
Data collection			
Space group	$P6_322$	$P6_322$	$C2$
Cell dimensions			
a, *b*, *c* (Å)	208.1, 208.1, 182.1	209.9, 209.9, 180.5	187.7, 170.1, 110.7
α, β, γ (°)	90.0, 90.0, 120.0	90.0, 90.0, 120.0	90.0, 117.3, 90.0
Resolution (Å)	30–4.50 (4.66–4.50)	30–3.55 (3.68–3.55)	50–3.15 (3.26–3.15)
R_{merge}	0.078 (0.592)	0.074 (0.498)	0.138 (0.496)
$I / \sigma I$	15.4 (4.9)	38.6 (6.5)	10.3 (2.9)
Completeness (%)	100.0 (100.0)	99.5 (100.0)	99.5 (98.8)
Redundancy	15.5 (10.9)	20.0 (18.5)	4.6 (4.5)
Refinement			
Resolution (Å)	30–4.52 (4.86–4.52)	30–3.55 (3.68–3.55)	20–3.15 (3.35–3.15)
No. reflections	14,115 (2,750)	28,487 (2,808)	52,452 (8,371)
R_{work} / R_{free}	0.326 (0.349) / 0.338 (0.362)	0.250 (0.342) / 0.283 (0.356)	0.231 (0.305) / 0.292 (0.365)
No. atoms			
Protein	4,135	4,006	16,229
Ligand/ion	28	28	64
B-factors			
Protein	271.5	138.8	70.3
Ligand/ion	324.8	161.6	96.2
R.m.s. deviations			
Bond lengths (Å)	0.009	0.009	0.009
Bond angles (°)	1.5	1.5	1.5

One crystal was used for each data set. Values in parentheses are for highest-resolution shell.

The interaction between MV-H and SLAM

The crystal structure shows four components of the binding interface (contact area of 1,050 Å^2) between MV-H and SLAM (sites 1–4, **Fig. 2a,b**). Site 1 is formed by salt bridges of Asp505 and Asp507 in the proposed acidic patch of MV-H to Lys77 and Arg90 of maSLAM-V. Site 2 is formed by salt bridges of MV-H Arg533 to MV-H Asp530 and maSLAM-V Glu123 as well as two hydrophobic interactions of MV-H Phe552 and Pro554 with maSLAM-V His61 and Val63. Site 3 is an intermolecular

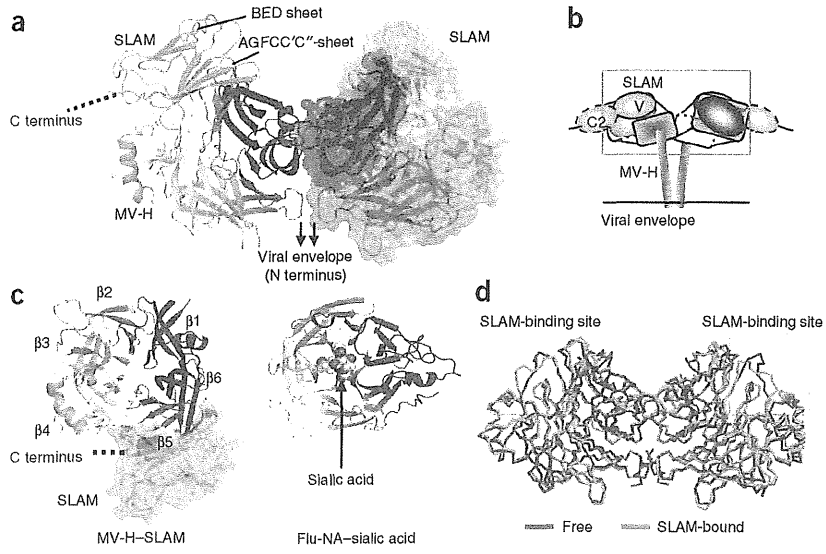

Figure 1 Overall structure of the MV-H–SLAM complex. (**a**) Side view of the MV-H–maSLAM-V complex. The MV-H head domain exhibits the six-bladed β-propeller fold (rainbow colors) and forms a homodimer. Monomer at left, ribbon diagram; monomer at right, surface diagram. SLAM-V (cyan) exhibits a typical β-sandwich structure with two β-sheets, BED and AGFCC'C". (**b**) Schematic of the homodimer of the MV-H–SLAM complex on the viral envelope. Gray cube, MV-H head domain with its top central pocket, which is probably covered by an N-linked sugar. Cyan ovals, V-set and C2-set Ig domains of SLAM. Box, area in a. (**c**) MV-H–SLAM and Flu-NA–sialic acid (PDB 1NSC) complexes as viewed downward through the top central pocket of respective β-propellers. MV-H and Flu-NA bind to their receptors using the side and the top of the β-propeller, respectively. (**d**) Side view of the free form (magenta) of the MV-H homodimer superimposed on that of the SLAM-bound form (cyan). Box, SLAM-binding site.

β-sheet assembled by the polypeptide backbones of the Pro191–Arg195 strand of MV-H (β6 sheet) and the Ser127–Phe131 strand of maSLAM-V. Site 4 is hydrophobic and has two components. The first is aromatic stacking of Tyr524, Tyr541, Tyr543 and Phe552 of MV-H with Phe119 and the Glu75-Arg130 salt bridge of maSLAM-V. The second involves hydrophobic interactions among Phe483, Tyr524, Tyr543 and Pro545 of MV-H and Asn72 and Val74 at the CC' loop region of maSLAM-V.

The host range of measles virus may be explained by key residues of SLAM at the interface shown by the crystal structure. All residues in contact with MV-H are conserved between marmoset and human SLAM except position 119 (phenylalanine in maSLAM and leucine in hSLAM)[9,11]. In contrast, murine SLAM, which cannot function as a receptor for measles virus[24], has multiple substitutions in this region, including two key residues, His61 and Arg130. hSLAMs mutated to contain Ser61 or Ser130 lose the ability to bind MV-H, as we detected by surface plasmon resonance (SPR) analysis (**Table 2**), and no longer support measles virus entry (**Fig. 2c**). Our previous study with chimeric and mutant SLAM proteins also showed the importance of His61 in measles virus receptor function of hSLAM[34]. The crystal structure shows that the aromatic ring of His61 of maSLAM makes a π-cation interaction with Arg533 of MV-H, which seems to stabilize the interaction of Arg533 with SLAM Glu123 (**Fig. 2b**, site 2). Arg130 on the G strand of maSLAM-V makes an intramolecular salt bridge with Glu75, located at the CC' loop, and also has stacking interactions with MV-H Phe552 and SLAM Phe119 (**Fig. 2b**, site 4). This may be the reason why the R130S substitution, but not the E75S substitution, abolishes the binding to MV-H and measles virus receptor function (**Table 2** and **Fig. 2c**). hSLAM E123S also does not bind MV-H and does not support measles virus infection. Mutations in other SLAM residues that interact with MV-H in the crystal structure less strongly affect binding to MV-H and measles virus infection (**Table 2**, **Fig. 2c** and **Supplementary Fig. 3a**).

From the structure of the SLAM-V monomer in the MV-H–maSLAM-V complex, we generated a model of the physiological SLAM-SLAM dimer (**Supplementary Fig. 4a**) based on the reported structure of the 2B4-CD48 heterodimer[35]. In this model, the homophilic binding interface is located on the FCC' β-sheet strands

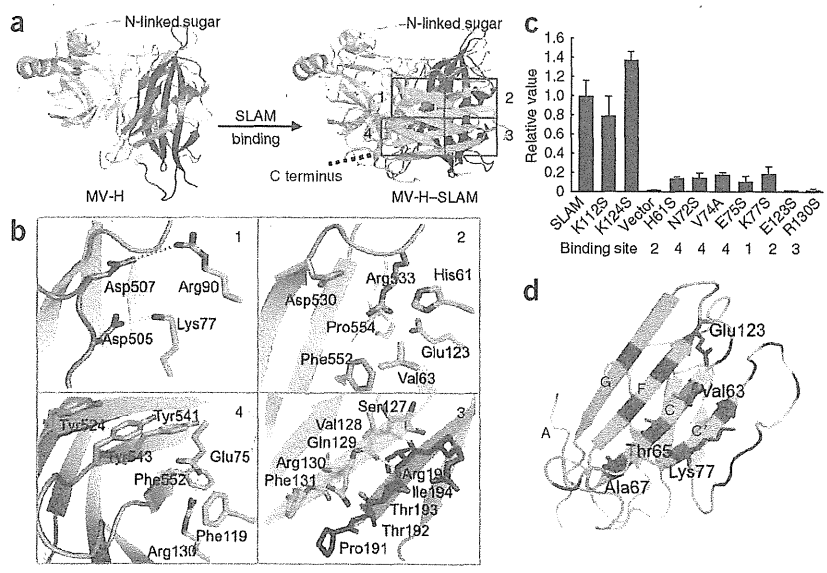

Figure 2 Interaction between MV-H and SLAM. (**a**) Side view of MV-H monomer (rainbow colors) bound (right) or unbound (left) to maSLAM-V (cyan) in a ribbon diagram. Top central pocket of the MV-H β-propeller is covered by an N-linked sugar. The four components of the binding interface are indicated (sites 1–4). (**b**) Detailed views of sites 1–4 (SLAM, cyan; MV-H, red or orange depending on the blade of β-propeller). (**c**) Measles virus receptor function of SLAM mutants as examined by measles virus entry assay. Representative of three separate experiments; error bars, s.d. (**d**) Residues assumed important for homophilic SLAM-SLAM binding (magenta) are mapped on the SLAM structure. They are located on the FCC' strands. Residues not involved in binding as determined by SPR analysis, blue.

Table 2 SPR analysis of SLAM mutants

Analyte	Ligand	Position of mutation	K_d (μM)[a]
MV-H	SLAM	—	0.52 ± 0.21
	SLAM H61S	Site 2	No binding
	SLAM N72S	Site 4	1.6 ± 0.17
	SLAM V74A	Site 4	2.0 ± 0.087
	SLAM E75S	Site 4	7.7 ± 1.1
	SLAM K77S	Site 1	1.7 ± 0.12
	SLAM E123S	Site 2	No binding
	SLAM R130S	Site 3	No binding
	SLAM N53Q	BC loop	1.1 ± 0.37
SLAM	SLAM	—	82 ± 3.4
	SLAM H61S	BC loop	107 ± 2.6
	SLAM V63A	C strand	No binding
	SLAM T65A	C strand	No binding
	SLAM A67D	C strand	No binding
	SLAM K77S	C′ strand	No binding
	SLAM E123S	F strand	No binding
	SLAM R130S	G strand	68 ± 0.88

Analyte, protein injected in solution; ligand, protein immobilized on CM5 chip. SPR sensorgrams, nonlinear fitting curves and other SLAM mutants examined are shown in **Supplementary Figure 3**. [a]K_d, mean ±s.d.

and the CC′ loop (**Fig. 2d** and **Supplementary Fig. 5a,b**). Present in the interface are Val63, Thr65, Ala67, Lys77 and Glu123. These residues are conserved in human, marmoset, cow, dog, sheep and mouse SLAM, except the one at position 63, which is leucine in SLAM of the last four species (**Supplementary Fig. 4b**). Substitutions of any of these residues in hSLAM caused a loss of homophilic binding (**Table 2** and **Supplementary Fig. 3b**), validating our structural model. Notably, the SLAM-SLAM binding interface largely overlaps with the MV-H–SLAM binding interface (Lys77 and Glu123). However, the affinity of the MV-H–SLAM interaction is >100-fold higher than that of the SLAM-SLAM interaction (**Table 2**). Thus, during measles virus entry, the MV-H–SLAM interaction should predominate over *cis* or *trans* SLAM-SLAM interactions on the host membrane.

MV-H tetramer

When we closely examined the crystal structures, we unexpectedly found two different potential tetrameric configurations of the MV-H–SLAM complex (forms I and II; **Fig. 3a,b**). The crystal structures at a resolution of 3.55 and 4.5 Å exhibit form I, whereas the structure at a resolution of 3.15 Å shows form II. Transient transfection of the full-length MV-H into HEK293T cells also produced tetramers, as we found with blue native PAGE (BN-PAGE) and immunoblotting (**Fig. 3c**). As has been shown for Newcastle disease virus (NDV)-HN[36] and PIV5-HN[29], the MV-H tetramer is a dimer of dimers that is arranged with two axes of two-fold symmetry. Monomers A and B form one dimer, and monomers C and D form another (**Fig. 3a,b,d**). Each dimer constituting a tetramer has essentially the same structure within and between the two forms. The overall configuration of MV-H form I is similar to those reported for NDV-HN, PIV5-HN and Flu-NA (**Supplementary Fig. 6**), although relative orientation of monomers in the dimer units varies substantially depending on the viral proteins. In form I, the MV-H monomers A and C largely form the interface of two dimers with a contact area of 1,312 Å^2 (**Fig. 3a,d**), and the N-terminal regions of four monomers are probably joined together, placing the stalks in the central axis (**Supplementary Fig. 6**). In contrast, the configuration of MV-H form II shifts the dimer-of-dimers interface to the boundary between monomers B and D (total contact area of 2,099 Å^2; **Fig. 3b,d**). This shifted dimer-of-dimers conformation would allow the stalk regions to move laterally, leaving a large central space (**Supplementary Fig. 6**). The residue at position 482 of MV-H mutated to obtain the structure at a resolution of 3.15 Å

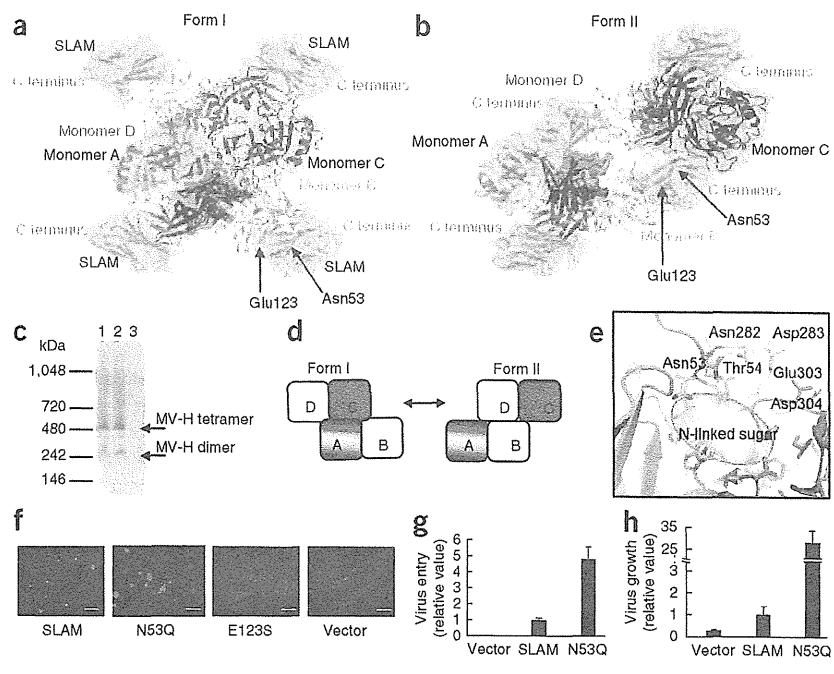

Figure 3 MV-H tetramer. (**a,b**) Two forms of MV-H dimer of dimers with each monomer bound to SLAM-V. MV-H monomers A (rainbow colors) and B (light pink) form one dimer, whereas monomers C (dark gray) and D (light gray) form another. Top view of form I, **a** (3.55 Å–resolution structure). Top view of form II, **b** (3.15 Å–resolution structure). (**c**) BN-PAGE analysis of full-length MV-H. Lanes 1 and 2, MV-H of the wild-type IC-B and Edmonston vaccine strains of measles virus, respectively. Lane 3, untransfected control cells. (**d**) Schematics of form I and form II MV-H tetramers. Colors of respective monomers are the same as in **a,b**. (**e**) The MV-H (green)-SLAM (cyan) interface containing SLAM Asn53 in form II. SLAM Asn53 with an N-linked sugar (gray oval) is located close to an acidic patch in MV-H monomer A or C. (**f**) Receptor function of SLAM mutants. Representative images of HEK293 cells transiently transfected with the plasmids encoding the indicated SLAM proteins or empty plasmid (vector) and infected with enhanced GFP–expressing recombinant measles virus without the fusion block peptide, as observed with a fluorescence microscope at 48 h after infection. Scale bars, 300 μm. (**g**) Entry efficiencies of SLAM proteins as examined by measles virus entry assay. Representative of three separate experiments; error bars, s.d. (**h**) Infection of HEK293 cells transiently transfected with plasmids encoding indicated SLAM proteins, with luciferase-expressing recombinant measles virus[18]. Luciferase activities were quantified at 24 h after infection. Error bars, s.d.

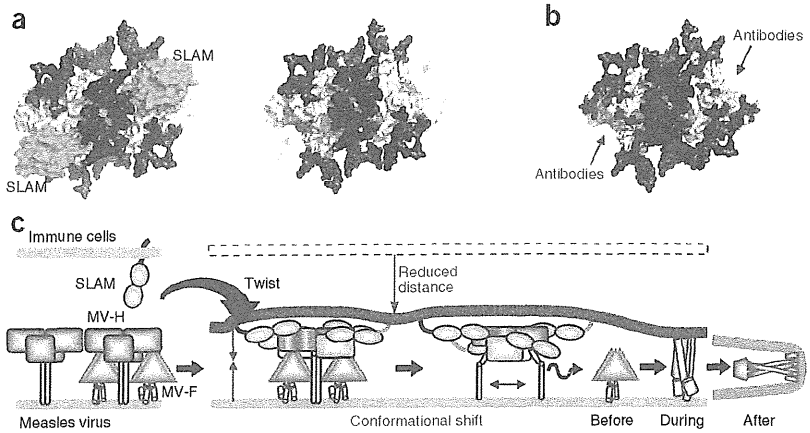

Figure 4 Structural basis of effectiveness of measles virus vaccine and a model of measles virus–induced membrane fusion. (**a**) Receptor-binding sites on MV-H. Left, structure of MV-H homodimer (gray) as viewed downward from top with potential N-linked sugars (black). SLAM (cyan) binds to the uncovered exposed surface of MV-H. Right, residues in orange are probably involved in interaction with putative epithelial cell receptor, based on site-directed mutagenesis of MV-H[19,20,27,28]. (**b**) Residues in red are epitopes of monoclonal antibodies to MV-H[39–41]. (**c**) The binding of MV-H to SLAM on an immune cell in a twisted 'head-to-head' orientation probably reduces the distance between the viral envelope and the cell membrane. The subsequent shift of the MV-H dimer-of-dimers conformation (form I to form II) may allow MV-F to undergo successive structural changes, leading to membrane fusion.

is not located at the dimer-of-dimers interface in either form I or II, suggesting that the substitution does not greatly affect the structure.

SLAM residues His61, Asn72, Val74, Glu75, Lys77, Glu123 and Arg130 mutated in the previous section are located close to MV-H in both forms I and II, whereas Asn53, a potential N-linked glycosylation site, is located at the interface between SLAM-V and MV-H monomer A (or C) only in form II (**Fig. 3a,b,e**). hSLAM N53Q has lower apparent molecular masses than wild-type hSLAM (data not shown), indicating that Asn53 is indeed used as an N-linked glycosylation site. hSLAM N53Q allows increased measles virus entry (**Fig. 3f,g**) and larger syncytium formation owing to enhanced cell-cell fusion (**Fig. 3f**), which leads to higher measles virus growth, compared with wild-type SLAM (**Fig. 3h**). Notably, this hSLAM mutant has similar affinity for direct binding to soluble MV-H (**Table 2**). One interpretation of these results is that the N53Q substitution facilitates stable formation of form II by removing carbohydrates between SLAM-V and MV-H and enhances membrane fusion after receptor binding. We also found a form II–like conformation in crystal packing of the reported structure of PIV3-HN, which contained a part of the stalk region in its construct[37] (**Supplementary Fig. 7**).

DISCUSSION

In this study, we have determined the crystal structure of MV-H bound to its primary receptor, SLAM. The structure shows the binding interface assembled by four sites (**Fig. 2b**). Mutagenesis studies have identified MV-H residues Ile194, Asp505, Asp507, Asp530, Arg533, Phe552 and Pro554 to be important for binding SLAM[27,28,38]. Our study confirms that these seven residues are indeed located at the interface. Three other residues of MV-H (Phe483, Tyr541 and Tyr543) are essential for infection of polarized epithelial cells, but not SLAM-positive immune cells[19,20]. These residues occur in site 4 in the crystal structure and do interact with SLAM, but on the basis of the mutagenesis data their contribution is probably not critical. The SLAM-binding interface provides a target for structure-based design of drugs to block the MV-H–SLAM interaction. For example, a hydrophobic pocket consisting of Tyr541, Tyr543, Phe552 and Pro554 at the center of the binding interface is also a part of the putative binding site for an unidentified epithelial cell receptor. Compounds targeted to this site may block both SLAM- and epithelial cell receptor–mediated measles virus infection. A recent study of the crystal structure of MV-H bound to the CD46 molecule, a receptor used only by vaccine strains of measles virus, has shown that two sequential proline residues on the protruding loop in the N-terminal domain of CD46 have a key role in the interaction with MV-H[23]. The authors suggest that a similar proline-proline motif found in SLAM (Pro88-Pro89) may be involved in the recognition of MV-H. However, our study shows that these residues are not directly in contact with MV-H, but rather precede Arg90 in site 1.

In our previous report, we proposed that N-linked sugars (present on Asn168, Asn187, Asn200 and Asn215) cover large surface areas of MV-H and therefore only a limited surface area is exposed for receptor and antibody binding[21]. Indeed, in both the SLAM-complexed (present study) and the uncomplexed structures of MV-H[21], the glycan attached to Asn215 seems to cover the large top pocket of the β-propeller head domain. The complexed crystal structure shows that a large part of the MV-H surface presumably left exposed is engaged by SLAM-V (**Fig. 4a**). Furthermore, the binding site for the epithelial cell receptor is probably located near the SLAM-binding site[19,20] (**Fig. 4a**), as is the binding site for the CD46 receptor[23] (**Supplementary Fig. 2**). Furthermore, the epitopes for most monoclonal antibodies to MV-H[39–41] map here as well (**Fig. 4b**). Thus, all receptors and most neutralizing antibodies bind to overlapping or closely located regions on the limited exposed surface of MV-H. This may explain why a single antibody can inhibit measles virus infection mediated by different receptors[18]. Furthermore, the inability of measles virus to mutate or mask its exposed receptor-binding face probably explains why the virus has never escaped immune responses induced by natural infection or vaccination, and still occurs in only a single serotype[3,42].

The free soluble MV-H (lacking a stalk) forms a homodimer[21]. Therefore, we did not expect that the MV-H–SLAM complex would exhibit a dimer of dimers (tetramer). Receptor binding could induce the formation of MV-H tetramers, as has been suggested for NDV tetramers[36]. However, our biochemical analysis shows that the full-length MV-H alone can form a tetramer (**Fig. 3c**). The stalk domain may induce tetramer formation. Indeed, free PIV5-HN containing a stalk forms a tetramer in solution and in crystals[29]. Henipavirus attachment G proteins containing a stalk also exist as tetrameric species[43]. Similarly, free intact MV-H molecules probably form dimers and tetramers on the viral envelope. This study suggests that receptor binding may facilitate MV-H tetramer formation even without the stalk region.

Partial disassembly of the dimer of dimers has been proposed as a mechanism of triggering paramyxovirus-mediated fusion, on the basis of crystal and electron microscopic structures of PIV5-HN[29,44]. Our results showing two forms of MV-H–SLAM tetramer

may provide the structural basis for such a model. Notably, both form I– and form II–like tetramer models can also be readily built by superimposing the reported MV-H–CD46 structure[23] on our structures of the MV-H–SLAM complex. Furthermore, we found that substitution of Lys54 abolishes measles virus receptor function of hSLAM without affecting its ability to bind MV-H (data not shown). Because maSLAM (used for crystallization) has a different residue at this position, we cannot determine exactly how Lys54 in hSLAM interacts with MV-H residues. However, we suppose that Lys54 is located close to MV-H in form II, but not in form I (**Fig. 3a,b,e**). Along with the data for the N53Q substitution (**Fig. 3f–h** and **Table 2**), the results suggest that form II has an important role in membrane fusion after receptor binding. Taken together, these results indicate that the shift of MV-H dimer of dimers could act as a mechanism of fusion triggering.

Our results may suggest the following sequence of events during measles virus–induced membrane fusion (**Fig. 4c**). The MV-H dimer of dimers is associated with the MV-F trimer on the viral envelope. At the host cell surface, the AGFCC′C″ β-sheet of SLAM-V binds to the side of the MV-H β-propeller, which is located upward from the virus surface because of the tilted orientation of the β-propeller. SLAM probably has straight V- and C2-set ectodomains, like those of other SLAM family receptors[45,46]. This structural arrangement inevitably renders the orientation of the V- and C2-set domains parallel rather than perpendicular in relation to the host membrane. The interaction substantially reduces the distance between the viral and host membranes (~140 Å if the stalk region of MV-H forms a straight α-helix[44,47]), setting the stage for the subsequent conformational change of MV-F and membrane fusion. Then, the configuration of the dimer of dimers may shift (from form I to form II), changing the orientation of the stalk regions, allowing MV-F to refold and interact with the target cell membrane and eventually leading to membrane fusion.

The dimer of dimers seems to have a weak interaction[29,44], and its conformational shift probably requires a small amount of energy and is probably induced by receptor binding. Such a shift of the attachment protein dimer of dimers may either actively induce the conformational change of the fusion protein required for membrane fusion or release the fusion protein from the clamp to facilitate its spontaneous conformational change, depending on the paramyxovirus species.

METHODS

Methods and any associated references are available in the online version of the paper at http://www.nature.com/nsmb/.

Accession codes. Protein Data Bank: Coordinates have been deposited for form I (4.5- and 3.55-Å resolution) and form II (3.15-Å resolution) of the MV-H–maSLAM complex (accession codes 3ALZ, 3ALW and 3ALX, respectively). GenBank: cDNA sequence of the measles virus Edmonston tag strain H protein, AB583749.

Note: Supplementary Information is available on the Nature Structural & Molecular Biology website.

ACKNOWLEDGMENTS

We thank the beamline staff of Photon Factory (Tsukuba, Japan) and SPring8 (Hyogo, Japan) for technical help during data collection. We also thank M.A. Billeter (Institute of Molecular Biology, University of Zürich) for reagents, M. Takeda, I. Tanaka, K. Inaba, K. Mihara, T. Oka, H. Aramaki, K. Tokunaga, M. Kajikawa, K. Kuroki and K. Sasaki for discussion and E.O. Saphire for reviewing the manuscript. This work was supported by grants from the Ministry of Education, Culture, Sports, Science and Technology of Japan and the Ministry of Health, Labor and Welfare of Japan. T.H. is supported by the Japan Society for the Promotion of Science Research Fellowship for Young Scientists.

AUTHOR CONTRIBUTIONS

T.H., K.M. and Y.Y. designed the research; T.H. and J.K. prepared and crystallized MV-H–SLAM complexes; T.H. and M.K. carried out binding, BN-PAGE and measles virus infection assays; T.H., T.O., N.M. and K.M. determined the crystal structures; T.H., K.M. and Y.Y. wrote the paper.

COMPETING FINANCIAL INTERESTS

The authors declare no competing financial interests.

Published online at http://www.nature.com/nsmb/.
Reprints and permissions information is available online at http://npg.nature.com/reprintsandpermissions/.

1. Bryce, J., Boschi-Pinto, C., Shibuya, K. & Black, R.E. WHO estimates of the causes of death in children. *Lancet* **365**, 1147–1152 (2005).
2. Moss, W.J. & Griffin, D.E. Global measles elimination. *Nat. Rev. Microbiol.* **4**, 900–908 (2006).
3. Griffin, D.E. in *Fields Virology* (eds. Knipe, D.M. *et al.*) 1551–1585 (Lippincott Williams & Wilkins, Philadelphia, 2007).
4. Harrison, S.C. Viral membrane fusion. *Nat. Struct. Mol. Biol.* **15**, 690–698 (2008).
5. Lamb, R.A. & Parks, G.D. in *Fields Virology* (eds. Knipe, D.M. *et al.*) 1449–1496 (Lippincott Williams & Wilkins, Philadelphia, 2007).
6. Iorio, R.M. & Mahon, P.J. Paramyxoviruses: different receptors—different mechanisms of fusion. *Trends Microbiol.* **16**, 135–137 (2008).
7. Smith, E.C., Popa, A., Chang, A., Masante, C. & Dutch, R.E. Viral entry mechanisms: the increasing diversity of paramyxovirus entry. *FEBS J.* **276**, 7217–7227 (2009).
8. Connolly, S.A., Leser, G.P., Jardetzky, T.S. & Lamb, R.A. Bimolecular complementation of paramyxovirus fusion and hemagglutinin-neuraminidase proteins enhances fusion: implications for the mechanism of fusion triggering. *J. Virol.* **83**, 10857–10868 (2009).
9. Tatsuo, H., Ono, N., Tanaka, K. & Yanagi, Y. SLAM (CDw150) is a cellular receptor for measles virus. *Nature* **406**, 893–897 (2000).
10. Yanagi, Y., Takeda, M., Ohno, S. & Hashiguchi, T. Measles virus receptors. *Curr. Top. Microbiol. Immunol.* **329**, 13–30 (2009).
11. Cocks, B.G. *et al.* A novel receptor involved in T-cell activation. *Nature* **376**, 260–263 (1995).
12. Schwartzberg, P.L., Mueller, K.L., Qi, H. & Cannons, J.L. SLAM receptors and SAP influence lymphocyte interactions, development and function. *Nat. Rev. Immunol.* **9**, 39–46 (2009).
13. Kiel, M.J. *et al.* SLAM family receptors distinguish hematopoietic stem and progenitor cells and reveal endothelial niches for stem cells. *Cell* **121**, 1109–1121 (2005).
14. Mavaddat, N. *et al.* Signaling lymphocytic activation molecule (CDw150) is homophilic but self-associates with very low affinity. *J. Biol. Chem.* **275**, 28100–28109 (2000).
15. Naniche, D. *et al.* Human membrane cofactor protein (CD46) acts as a cellular receptor for measles virus. *J. Virol.* **67**, 6025–6032 (1993).
16. Dörig, R.E., Marcil, A., Chopra, A. & Richardson, C.D. The human CD46 molecule is a receptor for measles virus (Edmonston strain). *Cell* **75**, 295–305 (1993).
17. Manchester, M., Liszewski, M.K., Atkinson, J.P. & Oldstone, M.B. Multiple isoforms of CD46 (membrane cofactor protein) serve as receptors for measles virus. *Proc. Natl. Acad. Sci. USA* **91**, 2161–2165 (1994).
18. Takeda, M. *et al.* A human lung carcinoma cell line supports efficient measles virus growth and syncytium formation via a SLAM- and CD46-independent mechanism. *J. Virol.* **81**, 12091–12096 (2007).
19. Tahara, M. *et al.* Measles virus infects both polarized epithelial and immune cells by using distinctive receptor-binding sites on its hemagglutinin. *J. Virol.* **82**, 4630–4637 (2008).
20. Leonard, V.H. *et al.* Measles virus blind to its epithelial cell receptor remains virulent in rhesus monkeys but cannot cross the airway epithelium and is not shed. *J. Clin. Invest.* **118**, 2448–2458 (2008).
21. Hashiguchi, T. *et al.* Crystal structure of measles virus hemagglutinin provides insight into effective vaccines. *Proc. Natl. Acad. Sci. USA* **104**, 19535–19540 (2007).
22. Colf, L.A., Juo, Z.S. & Garcia, K.C. Structure of the measles virus hemagglutinin. *Nat. Struct. Mol. Biol.* **14**, 1227–1228 (2007).
23. Santiago, C., Celma, M.L., Stehle, T. & Casasnovas, J.M. Structure of the measles virus hemagglutinin bound to the CD46 receptor. *Nat. Struct. Mol. Biol.* **17**, 124–129 (2010).
24. Ono, N., Tatsuo, H., Tanaka, K., Minagawa, H. & Yanagi, Y. V domain of human SLAM (CDw150) is essential for its function as a measles virus receptor. *J. Virol.* **75**, 1594–1600 (2001).
25. Reeves, P.J., Callewaert, N., Contreras, R. & Khorana, H.G. Structure and function in rhodopsin: high-level expression of rhodopsin with restricted and homogeneous N-glycosylation by a tetracycline-inducible N-acetylglucosaminyltransferase I-negative HEK293S stable mammalian cell line. *Proc. Natl. Acad. Sci. USA* **99**, 13419–13424 (2002).

26. Evans, E.J. *et al.* Crystal structure and binding properties of the CD2 and CD244 (2B4)-binding protein, CD48. *J. Biol. Chem.* **281**, 29309–29320 (2006).
27. Massé, N. *et al.* Measles virus (MV) hemagglutinin: evidence that attachment sites for MV receptors SLAM and CD46 overlap on the globular head. *J. Virol.* **78**, 9051–9063 (2004).
28. Vongpunsawad, S., Oezgun, N., Braun, W. & Cattaneo, R. Selectively receptor-blind measles viruses: Identification of residues necessary for SLAM- or CD46-induced fusion and their localization on a new hemagglutinin structural model. *J. Virol.* **78**, 302–313 (2004).
29. Yuan, P. *et al.* Structural studies of the parainfluenza virus 5 hemagglutinin-neuraminidase tetramer in complex with its receptor, sialyllactose. *Structure* **13**, 803–815 (2005).
30. Bowden, T.A. *et al.* Structural basis of Nipah and Hendra virus attachment to their cell-surface receptor ephrin-B2. *Nat. Struct. Mol. Biol.* **15**, 567–572 (2008).
31. Xu, K. *et al.* Host cell recognition by the henipaviruses: crystal structures of the Nipah G attachment glycoprotein and its complex with ephrin-B3. *Proc. Natl. Acad. Sci. USA* **105**, 9953–9958 (2008).
32. Varghese, J.N., Laver, W.G. & Colman, P.M. Structure of the influenza virus glycoprotein antigen neuraminidase at 2.9 A resolution. *Nature* **303**, 35–40 (1983).
33. Burmeister, W.P., Ruigrok, R.W. & Cusack, S. The 2.2 A resolution crystal structure of influenza B neuraminidase and its complex with sialic acid. *EMBO J.* **11**, 49–56 (1992).
34. Ohno, S., Seki, F., Ono, N. & Yanagi, Y. Histidine at position 61 and its adjacent amino acid residues are critical for the ability of SLAM (CD150) to act as a cellular receptor for measles virus. *J. Gen. Virol.* **84**, 2381–2388 (2003).
35. Velikovsky, C.A. *et al.* Structure of natural killer receptor 2B4 bound to CD48 reveals basis for heterophilic recognition in signaling lymphocyte activation molecule family. *Immunity* **27**, 572–584 (2007).
36. Zaitsev, V. *et al.* Second sialic acid binding site in Newcastle disease virus hemagglutinin-neuraminidase: implications for fusion. *J. Virol.* **78**, 3733–3741 (2004).
37. Lawrence, M.C. *et al.* Structure of the haemagglutinin-neuraminidase from human parainfluenza virus type III. *J. Mol. Biol.* **335**, 1343–1357 (2004).
38. Navaratnarajah, C.K. *et al.* Dynamic interaction of the measles virus hemagglutinin with its receptor signaling lymphocytic activation molecule (SLAM, CD150). *J. Biol. Chem.* **283**, 11763–11771 (2008).
39. Hu, A., Sheshberadaran, H., Norrby, E. & Kovamees, J. Molecular characterization of epitopes on the measles virus hemagglutinin protein. *Virology* **192**, 351–354 (1993).
40. Fournier, P. *et al.* Antibodies to a new linear site at the topographical or functional interface between the haemagglutinin and fusion proteins protect against measles encephalitis. *J. Gen. Virol.* **78**, 1295–1302 (1997).
41. Ertl, O.T., Wenz, D.C., Bouche, F.B., Berbers, G.A. & Muller, C.P. Immunodominant domains of the Measles virus hemagglutinin protein eliciting a neutralizing human B cell response. *Arch. Virol.* **148**, 2195–2206 (2003).
42. Ruigrok, R.W. & Gerlier, D. Structure of the measles virus H glycoprotein sheds light on an efficient vaccine. *Proc. Natl. Acad. Sci. USA* **104**, 20639–20640 (2007).
43. Bossart, K.N. *et al.* Receptor binding, fusion inhibition, and induction of cross-reactive neutralizing antibodies by a soluble G glycoprotein of Hendra virus. *J. Virol.* **79**, 6690–6702 (2005).
44. Yuan, P., Leser, G.P., Demeler, B., Lamb, R.A. & Jardetzky, T.S. Domain architecture and oligomerization properties of the paramyxovirus PIV 5 hemagglutinin-neuraminidase (HN) protein. *Virology* **378**, 282–291 (2008).
45. Chothia, C. & Jones, E.Y. The molecular structure of cell adhesion molecules. *Annu. Rev. Biochem.* **66**, 823–862 (1997).
46. Cao, E. *et al.* NTB-A receptor crystal structure: insights into homophilic interactions in the signaling lymphocytic activation molecule receptor family. *Immunity* **25**, 559–570 (2006).
47. Paal, T. *et al.* Probing the spatial organization of measles virus fusion complexes. *J. Virol.* **83**, 10480–10493 (2009).

ONLINE METHODS

Construction of expression plasmids. The DNA fragments encoding the MV-H head domain (Asp149–Arg617 or Ser184–Arg617) were amplified by PCR using the p(+)MV2A (a gift from M.A. Billeter) containing the antigenomic full-length cDNAs of the Edmonston tag strain of measles virus[48] as a template. These amplified fragments were cloned into a derivative of the expression vector pCA7 (ref. 49) as described[21]. This derivative vector contains the signal and His_6 tag sequences up- and downstream of the protein-coding sequence, respectively, and allows high-level expression of secreted proteins. The fragment encoding maSLAM-V including the authentic signal sequence (Met1–Gln140) was amplified by PCR from the pCAGB95aSLAM plasmid that contains the full-length cDNA of maSLAM[9], and cloned into pCA7 that contains a His_6 tag sequence downstream of the protein-coding sequence. To express single-chain MV-H–maSLAM-V fusion proteins, a $(Gly\text{-}Gly\text{-}Gly\text{-}Ser)_3$ linker was inserted between the sequence encoding the MV-H head domain (Ser184–Thr607) and that encoding maSLAM-V (Met30–Gln140). To increase stability and solubility of the expressed proteins, several mutations were introduced at various positions of the fusion construct. The crystals examined in this study were obtained using the constructs in which mutations were introduced at position 482 of MV-H (L482R) and/or positions 102 and 108 of maSLAM-V (N102H R108Y). The L482R substitution was used, as change from leucine to a basic residue at position 482 of MV-H increases SLAM-dependent cell fusion (data not shown), and this substitution has been found in a clinical isolate of measles virus (genotype D1). The N102H and R108Y substitutions of maSLAM-V were adopted to remove an N-linked glycosylation site and prevent the charge repulsion, respectively, based on the structure at a resolution of 4.5 Å. Tyrosine was used to replace arginine at position 108, as CD48 has tyrosine at the corresponding position. For binding assays, a fragment encoding the ectodomain of hSLAM (Gly26–Ala239) was amplified by PCR using the pCAGSLAM containing the full-length cDNA of hSLAM[9], and cloned into pCA7 containing the signal and influenza virus hemagglutinin tag sequences and biotinylation tag sequence up- and downstream of the protein-coding sequence, respectively. For measles virus entry and infection assays, a fragment encoding hSLAM (Gly26–Ser335) was amplified and cloned into pCA7 containing the signal and hemagglutinin tag sequences upstream of the protein-coding sequence.

Expression, purification and modification of proteins. To prepare soluble proteins, expression plasmids encoding the appropriate proteins were transiently transfected using polyethyleneimine, together with the plasmid encoding the SV40 large T antigen, into 90% confluent HEK293S GnTI$^-$ cells[21,25]. The cells were cultured in DMEM supplemented with 10% (v/v) FBS (FBS), L-glutamine and nonessential amino acids (Gibco). The concentration of FBS was lowered to 2% (v/v) immediately after transfection. Supernatants containing the expressed proteins were harvested 5 d after transfection, and mixed with the Ni^{2+}-NTA affinity column binding buffer (50 mM NaH_2PO_4, 150 mM NaCl, 10 mM imidazole, pH 8.0). The proteins were purified via Ni^{2+}-NTA affinity, followed by Superdex 200GL 10/300 (GE Healthcare) gel filtration chromatography. To introduce methylation in lysine residues, the purified protein was treated with 20 mM dimethyl-boron and 40 mM formaldehyde at 4 °C overnight, and repurified by size-exclusion chromatography. For SPR analysis, expression plasmids encoding the proteins with the biotinylation tag at the C terminal were transiently transfected into HEK293 cells cultured in OPTI-MEM medium. At 4 d after transfection, the culture media were centrifuged, sterile-filtered, and treated with biotin-protein ligase (Avidity) in 20 mM Tris-HCl, pH 8.0 at 30 °C for 2 h. Supernatants containing the biotinylated proteins were subsequently dialyzed against HEPES-buffered saline (HBS)-P buffer (10 mM HEPES, 150 mM NaCl, 0.005% (v/v) surfactant P20, pH 7.4) (GE Healthcare) and injected onto the streptavidin-attached sensor chip on which only the biotinylated proteins were immobilized.

Crystallization of MV-H in complex with SLAM-V. Crystals were grown by the sitting- or floating-drop vapor diffusion using Fluorinert (Hampton Research) at 20 °C (ref. 50). A 1:1 mixture of $MV\text{-}H_{149\text{–}617}$ and $maSLAM\text{-}V_{1\text{–}140}$ containing 0.2 µl each of protein (9.3 mg ml^{-1}, in 20 mM imidazole, pH 8.0, 100 mM NaCl) and mother liquor (0.1 M MES, pH 6.5, 0.75 M Li_2SO_4) was set up for crystallization. Crystals of this complex diffract only to a resolution of 4.5 Å. Drops of the single-chain $MV\text{-}H_{184\text{–}607}$–$maSLAM_{30\text{–}140}$ N102H R108Y) containing 1 µl each of protein (12.7 mg ml^{-1}, in 20 mM imidazole, pH 8.0, 100 mM NaCl) and mother liquor (0.1 M imidazole pH 5.8, 0.5 M $(NH_4)_2SO_4$, 0.7 M Li_2SO_4, 3% (v/v) ethylene glycol) produced crystals that diffract to a resolution of 3.55 Å. To obtain higher-resolution structures, the single-chain $MV\text{-}H_{184\text{–}607}$ L482R–$maSLAM\text{-}V_{30\text{–}140}$ N102H R108Y) complex was prepared. Crystallization was achieved in the solution containing 1 µl each of protein (14.0 mg ml^{-1}, in 20 mM imidazole, pH 8.0, 100 mM NaCl) and mother liquor (0.1 M imidazole, pH 8.3, 0.5 M $(NH_4)_2SO_4$, 0.7 M Li_2SO_4, 0.05 M lithium acetate, 1% (v/v) ethylene glycol). These crystals diffract to a resolution of 3.15 Å.

Structure determination, binding analysis, assays for measles virus entry and infection and BN-PAGE are described in the **Supplementary Methods.**

48. Radecke, F. *et al.* Rescue of measles viruses from cloned DNA. *EMBO J.* **14**, 5773–5784 (1995).
49. Takeda, M. *et al.* Long untranslated regions of the measles virus M and F genes control virus replication and cytopathogenicity. *J. Virol.* **79**, 14346–14354 (2005).
50. Adachi, H. *et al.* Application of a two-liquid system to sitting-drop vapour-diffusion protein crystallization. *Acta Crystallogr. D Biol. Crystallogr.* **59**, 194–196 (2003).

doi:10.1038/nsmb.1969

frontiers in MICROBIOLOGY

REVIEW ARTICLE
published: 16 December 2011
doi: 10.3389/fmicb.2011.00247

Measles virus hemagglutinin: structural insights into cell entry and measles vaccine

Takao Hashiguchi [1,2]*, Katsumi Maenaka [3,4] and Yusuke Yanagi [1]

[1] Department of Virology, Faculty of Medicine, Kyushu University, Fukuoka, Japan
[2] Department of Immunology and Microbial Science, The Scripps Research Institute, La Jolla, CA, USA
[3] Laboratory of Biomolecular Science, Hokkaido University, Sapporo, Japan
[4] Core Research for Evolutional Science and Technology, Japan Science and Technology Agency, Saitama, Japan

Edited by:
Akio Adachi, The University of Tokushima, Japan

Reviewed by:
Kaoru Takeuchi, University of Tsukuba, Japan
Hak Hotta, Kobe University, Japan

***Correspondence:**
Takao Hashiguchi, Department of Virology, Kyushu University, Fukuoka 812-8582, Japan; Department of Immunology, The Scripps Research Institute, 10550 North Torrey Pines Road, La Jolla, CA 92037, USA.
e-mail: takaoh@scripps.edu

Measles is one of the most contagious viral diseases, and remains a major cause of childhood morbidity and mortality worldwide. The measles virus (MV), a member of the family *Paramyxoviridae*, enters cells through a cellular receptor, the signaling lymphocyte activation molecule (SLAM), CD46 or nectin-4. Entry is mediated by two MV envelope glycoproteins, the hemagglutinin (H) and the fusion (F) protein. The H protein mediates receptor attachment, while the F protein causes membrane fusion. The interaction between the H and F proteins is essential to initiate the cell entry process. Recently determined crystal structures of the MV-H protein unbound and bound to SLAM or CD46 have provided insights into paramyxovirus entry and the effectiveness of measles vaccine.

Keywords: measles virus, hemagglutinin, structure, fusion, entry, measles vaccine, glycoprotein, receptor

INTRODUCTION

Measles virus (MV), the agent that causes measles, is an enveloped, non-segmented, negative-strand RNA virus, a member of the genus *Morbillivirus*, the family *Paramyxoviridae* (Griffin, 2007). Paramyxoviruses also include, among others, mumps virus, Newcastle disease virus (NDV), human parainfluenza viruses (hPIV), and emerging Hendra virus (HeV) and Nipah virus (NiV), members of the genus *Henipavirus* (Lamb and Parks, 2007). MV enters cells through membrane fusion in a pH-independent manner, like other paramyxoviruses. MV possesses two glycoproteins on its envelope, an attachment protein hemagglutinin (H) (MV-H) and a fusion (F) protein (MV-F) (Griffin, 2007). MV-H and MV-F form hetero-oligomer, which is required to induce membrane fusion. Upon receptor binding, MV-H is thought to undergo a conformational change, which in turn would trigger a structural rearrangement of MV-F from the metastable pre-fusion form to the intermediate and post-fusion forms (Plemper et al., 2011). This conformational change of MV-F would drive the fusion between the viral envelope and the host cell membrane. Currently, the detailed structural organization of MV-H and MV-F remains elusive.

The paramyxovirus attachment proteins are classified into three groups based on their functions, the hemagglutinin–neuraminidase (HN) protein, the H protein, and the G protein. Although these attachment proteins may have a common assembly process, their interaction with the F protein may be viral species-dependent, and different paramyxoviruses may use different strategies for fusion activation (Lamb and Parks, 2007; Iorio and Mahon, 2008; Connolly et al., 2009; Smith et al., 2009; Plemper et al., 2011). Among paramyxoviruses, only those belonging to the genera *Morbillivirus* and *Henipavirus* recognize protein receptors expressed on the target cell surface. This is in marked contrast to most other members of the family *Paramyxoviridae*, which contain the neuraminidase domain in their HN proteins and recognize sialic acid-containing receptors.

Three protein molecules have been identified as MV receptors, the signaling lymphocyte activation molecule (SLAM), CD46, and nectin-4. On the other hand, NiV and HeV utilize as receptors ephrin (Eph) B2 and EphB3, which belong to the highly conserved Eph family of tyrosine kinase receptors (Bonaparte et al., 2005; Negrete et al., 2005, 2006). Although both MV and henipaviruses recognize protein receptors, there is a large structural difference between MV-H and henipavirus G proteins (Bowden et al., 2010). The G proteins exhibit a structural-fold property closer to that of HN proteins. This suggests that MV-H and henipavirus G proteins have independently evolved the ability to recognize protein receptors.

One clinical isolate obtained from a child in 1954 known as the Edmonston strain gave rise to the majority of current MV vaccine strains (Katz, 2009). After 50 years, its progeny (Edmonston lineage) are still effective as live attenuated vaccines. It is estimated that more than 4.5 million measles deaths have been prevented annually through implementation of the vaccination strategies developed by WHO and UNISEF (Bellini and Rota, 2011).

Here, we review recent advances in our understanding of MV entry, based on crystal structures of MV-H–receptor complexes as well as functional studies. We compare the attachment protein-receptor complex of MV with those of other paramyxoviruses, and provide a general principle of paramyxovirus entry. We also discuss why MV has only one major serotype and why our current

MV vaccine prepared more than five decades ago from a single strain is still effective.

MV RECEPTORS

CD46

Currently, three receptors are identified, which facilitate MV entry. CD46 (also called membrane cofactor protein) is the first MV receptor discovered by two groups independently in 1993 (Dorig et al., 1993; Naniche et al., 1993). CD46 is a type I membrane protein that belongs to the regulators of complement activation (RCA) family. CD46 comprises an N-terminal signal sequence, four short consensus repeats (SCR1–SCR4), a transmembrane region, and a C-terminal cytoplasmic tail. Each SCR module contains ~60 amino acids that fold into a compact β-barrel structure (Persson et al., 2010). N-terminal domains SCR1 and SCR2 participate in the interaction with MV-H (Santiago et al., 2010).

CD46 is expressed on all nucleated human cells, and acts as a cofactor in the proteolytic inactivation of C3b and C4b by factor I. Monkey, but not human, erythrocytes express CD46, allowing hemagglutination by MV (Cole et al., 1985; Kemper and Atkinson, 2009). Interestingly, only vaccine and laboratory-adapted strains of MV can utilize CD46 as a receptor, while clinically isolated MV strains employ different receptors for entry.

SIGNALING LYMPHOCYTE ACTIVATION MOLECULE

Measles viruses were found to be efficiently isolated from clinical specimens by using the marmoset B cell line B95a or other human B cell lines (Kobune et al., 1990; Schneider-Schaulies et al., 1995). Further, MVs obtained using these cell lines were unable to downregulate CD46 or induce cell-to-cell fusion in CD46-positive cell lines (Lecouturier et al., 1996; Bartz et al., 1998; Tanaka et al., 1998). These observations suggested the presence of MV receptor(s) other than CD46. In 2000, SLAM (also known as CD150) was identified as a principal cellular receptor for all MV strains (Tatsuo et al., 2000).

Signaling lymphocyte activation molecule, a member of the immunoglobulin (Ig) superfamily, is a type I membrane protein that possesses an N-terminal signal sequence, two Ig-like domains (V-set and C2-set), a transmembrane region, and a cytoplasmic tail (Cocks et al., 1995). Each Ig-like domain has ~110 amino acid residues. Only the membrane-distal V-set domain is necessary and sufficient for MV-H binding. The V domain is comprised of the BED and AGFCC′C″ β-sheet, which utilize a Cys32–Cys132 disulfide bond to stabilize the A–G interstrand interaction (Hashiguchi et al., 2011).

In humans, SLAM is expressed on thymocytes, activated lymphocyte, mature dendritic cells, macrophages, and platelets. However, it is absent from monocytes, natural killer cells, and granulocytes (Schwartzberg et al., 2009). The distribution of SLAM nicely explains the tropism and immunosuppressive nature of MV (Yanagi et al., 2009).

NECTIN-4

Although epithelial cells do not express SLAM, MV antigens, and syncytia have been observed in the epithelia of various organs from measles patients and experimentally infected monkeys. It was found that a human lung adenocarcinoma cell line NCI-H358 supports SLAM- and CD46-independent MV infection (Takeda et al., 2007). Furthermore, several polarized epithelial cell lines have been reported to be susceptible to MV (Takeda et al., 2007; Leonard et al., 2008; Tahara et al., 2008). Together, these data hinted at the presence of a third MV receptor.

Recent studies have identified nectin-4 as an epithelial cell receptor (Muhlebach et al., 2011; Noyce et al., 2011). Human nectin-4 is expressed mainly in placenta cells, and to a lesser degree in trachea cells (Reymond et al., 2001). Nectin-4 is a member of the poliovirus receptor-like proteins (PVRLs), which are adhesion receptors of the Ig superfamily. Similar to SLAM, this type I membrane protein contains an N-terminal signal sequence, three Ig-like domains (V-set and two C2-set), a transmembrane region, and a cytoplasmic tail. Each Ig-like domain is predicted to be ~105 amino acid residues. Both wild type and the Edmonston lineage MV strains can use nectin-4 as a receptor.

MV-H PROTEIN

The MV-H is a type II membrane glycoprotein comprised of an N-terminal cytoplasmic tail, a transmembrane region, a stalk, and a C-terminal receptor-binding head domain. The head domain of MV-H exhibits a six-bladed β-propeller fold, a feature conserved among all head domains of paramyxovirus attachment proteins thus far crystallized (Colf et al., 2007; Hashiguchi et al., 2007). Without a neuraminidase domain, MV-H targets protein receptors, SLAM, CD46, and nectin-4. The difference in receptor preference between H and HN proteins reflects the difference in their head domain structures (see below).

Crystal structure of the MV-H head domain reveals a top pocket reminiscent of the sialic acid binding cavity found in both HN proteins and the neuraminidase (NA) of influenza virus (Flu). However, the pocket in MV-H is enlarged and lacks several key residues that contribute to sialic acid binding. In addition, the N-linked sugar at position 215 of MV-H (located at the rim of the pocket) renders the top pocket inaccessible to sialic acid, antibodies or other molecules. The MV-H head domain exhibits a cubic shape, and forms a homodimer (Hashiguchi et al., 2007). Two neighboring N-linked sugars at position 200 (one each from both monomers), located at the homodimer interface, likely block access to the region, which in HN of NDV, has been proposed to contain a second sialic acid binding site. Similarly, HNs of hPIV3 and PIV5 do not contain a second sialic acid binding site due to N-linked sugar at Asn523 and Asn497, respectively.

INTERACTION BETWEEN MV-H AND RECEPTORS

Mutagenesis studies have suggested that receptor-binding sites on MV-H are located on the side of the β-propeller, which was subsequently confirmed by the crystal structures of MV-H complexed with SCR1 and SCR2 of CD46 or with the V domain of SLAM (**Figure 1A**; Santiago et al., 2010; Hashiguchi et al., 2011). By contrast, attachment proteins of NDV, hPIV3, and PIV5, NA of Flu and G proteins of NiV and HeV utilize the top pocket of the β-propeller structure for binding to their corresponding receptors or ligand (**Figure 1B**; Burmeister et al., 1992; Crennell et al., 2000; Lawrence et al., 2004; Yuan et al., 2005; Bowden et al., 2008; Xu et al., 2008).

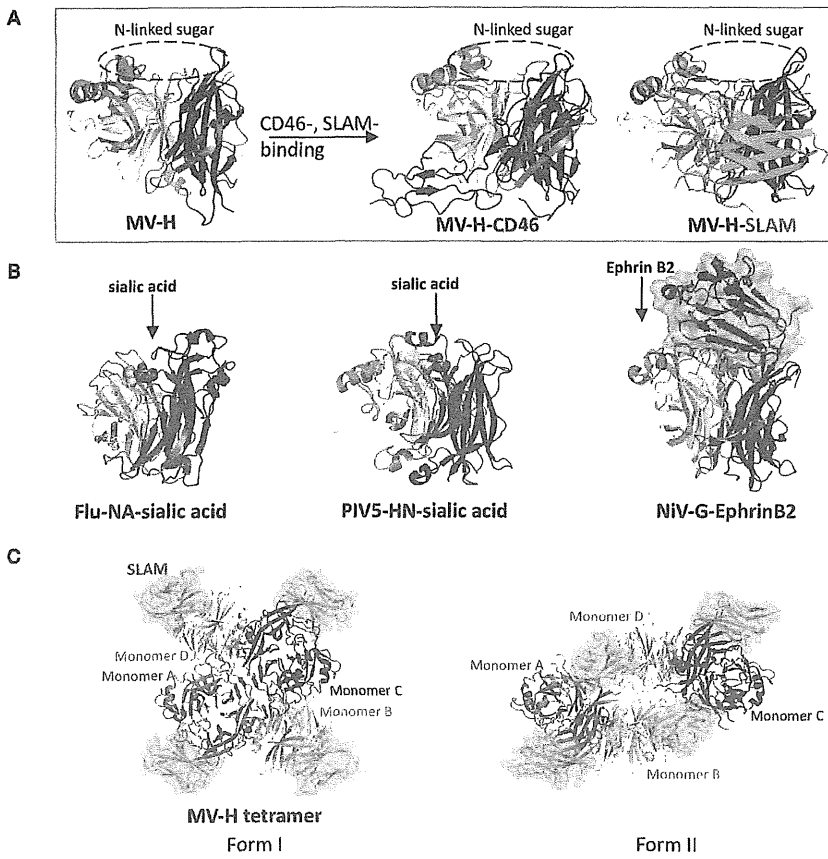

FIGURE 1 | Structures of viral glycoproteins exhibiting the β-propeller fold unbound or bound to their receptors or ligand. (A) Side view of the MV-H monomer (rainbow colors) unbound (left) or bound to CD46 (middle) or SLAM (right). CD46 (purple) and SLAM (cyan) are indicated in a ribbon diagram. The top pocket of the MV-H monomer is masked by N-linked sugar. **(B)** Side views of Flu-NA bound to sialic acid (left), PIV5-HN bound to sialic acid (middle), and NiV-G bound to ephrin B2 (right). Sialic acid (white and red) is indicated as sphere models, whereas ephrin B2 (black) is shown in surface presentation. **(C)** Top views of two forms of MV-H tetramer with each monomer bound to SLAM (cyan). MV-H monomers A (green) and B (light green) form one dimer, whereas monomers C (black) and D (gray) form another.

Crystal structure of MV-H bound to CD46 reveals that β-sheet 4 (β4) and β5 of the β-propeller structure interact with SCR1 and SCR2 of CD46 (**Figure 1A**; Santiago et al., 2010). Key residues Tyr481 and Gly546 on MV-H make hydrogen bonds with the main chain oxygen group of Cys65 and the main chain amino group of Glu63 on CD46, respectively. Furthermore, a serine-to-glycine mutation at position 546 on MV-H (found in some CD46-using MV strains) likely increases flexibility of the β5s3–β5s4 region, which is favorable for CD46 binding. Pro38 and Pro39 on CD46 are sandwiched between β4 residues Leu464 and Leu500 and β5 residues Tyr541 and Tyr543 on MV-H, while Tyr67 on CD46 makes a hydrophobic interaction with Val451 on MV-H. The interaction between MV-H and CD46 is relatively week (K_d, 2.2 μM; Hashiguchi et al., 2007).

Crystal structure of MV-H in complex with SLAM shows that β4–6 and loop regions on the lateral surface of the MV-H β-propeller structure interact with GFCC′C″ region of the SLAM-V domain (**Figure 1A**; Hashiguchi et al., 2011). This interaction is also confirmed by functional assays, surface plasmon resonance and infectious assay *in vitro*. Salt bridges formed by residues Asp530 and Arg533 on MV-H and Glu123 on SLAM play a key role in stabilizing the MV-H–SLAM complex. An intermolecular β-sheet, comprised of residues Pro191-Arg195 (β6) of MV-H and residues Ser127-Phe131 (G sheet) of SLAM-V, further stabilizes the MV-H–SLAM complex. Mouse SLAM does not contain the MV-H-interacting key residues, including His61 and Arg130, and therefore does not act as a MV receptor (Ono et al., 2001). Although SLAM interacts with another SLAM through its V domain, the affinity of SLAM–SLAM interaction (K_d of ~200 μM) is over 400-fold lower than that of the MV-H–SLAM interaction (K_d of 0.29 ~ 0.43 μM; Hashiguchi et al., 2007). Therefore, upon MV infection, SLAM preferentially interacts with MV-H rather than adjacent SLAM.

Mutagenesis studies have mapped nectin-4 binding sites in a region partly shared by SLAM-binding sites (Leonard et al., 2008; Tahara et al., 2008). Amino acids in this region are highly conserved

among morbilliviruses, whereas CD46 binding sites are not. Thus, it is likely that many morbilliviruses utilize this region of the H protein to infect immune and epithelial cells.

Like other paramyxovirus attachment proteins, MV-H forms a homodimer (or tetramer, see below). Interestingly, two monomers forming the MV-H dimer are highly tilted from each other, in contrast to other paramyxovirus attachment proteins (Hashiguchi et al., 2007). As a result, the receptor-binding sites on MV-H (located at the side of the β-propeller) are oriented upward in such a way that they are readily accessible to cellular receptors. This structural property and the inaccessibility of the top pocket due to N-linked sugar at position 215 account for the difference in receptor-binding sites between MV-H and other paramyxovirus attachment proteins.

MV-H TETRAMER AND MEMBRANE FUSION TRIGGERING

The mechanism by which receptor-binding leads to F protein-mediated membrane fusion is not well understood. However, crystal structures of MV-H–CD46 and MV-H–SLAM have also provided clues for this intriguing process (Santiago et al., 2010; Hashiguchi et al., 2011). No large structural change is observed in the MV-H monomer between receptor-free and receptor-bound forms. Furthermore, the relative orientation of two monomers in the MV-H dimer also remains essentially identical before and after receptor binding (r.m.s. deviation of 1.95 Å for 751 Ca atoms in MV-H–SLAM; r.m.s. deviation of 1.33 Å for 791 Ca atoms in MV-H–CD46).

Interestingly, crystal structures of the MV-H–SLAM complex reveal two different tetrameric configurations (dimer of dimers), form I and form II (**Figure 1C**; Hashiguchi et al., 2011). The tetrameric formation of MV-H is also detected by native PAGE and immunoblotting when the full-length MV-H is transiently expressed in cells. Recently reported crystal structures of NDV and PIV5 also reveal a four-helix bundle stalk (Bose et al., 2011; Yuan et al., 2011). MV-H monomers A and B form one dimer, while monomers C and D form another, and SLAM is bound to each MV-H monomer. Form I exhibits a conformation similar to previously reported head domains of NDV-HN, hPIV3-HN, PIV5-HN, and Flu-NA, although the relative position of monomers in the dimer units varies depending on the viral protein. In form II, a shift in the dimer of dimers occurs, enabling SLAM to bridge two neighboring monomers. Monomers A and C form the dimer–dimer interface in form I (contact area of 1.312 Å), whereas monomers B and D mainly form the dimer–dimer interface in form II (contact area of 2.099 Å). Based on these structural features, we propose the following fusion triggering mechanism. Upon the virus–cell interaction, the MV-H–SLAM complex in form I is formed. This structure renders the orientation of SLAM parallel rather than perpendicular in relation to the host membrane, and substantially reduces the distance between viral envelope and host membrane. This may prepare the environment suitable for subsequent conformational changes of MV-H and MV-F. The ensuing conformational shift of MV-H from form I to form II reorganizes the stalk region, allowing MV-F to refold and interact with the target cell membrane (Hashiguchi et al., 2011).

In a recent study, disulfide bonds were introduced at the protein interface to covalently anchor the two head domains in the MV-H dimer, leading to the block of its fusion-support activity (Navaratnarajah et al., 2011). The authors proposed that the two head domains in an MV-H dimer twist relative to each other upon receptor binding, which triggers membrane fusion. However, twisting of the head domains is not consistent with crystal structures of MV-H bound and unbound to receptors (Hashiguchi et al., 2007, 2011; Santiago et al., 2010). These introduced disulfide bonds might somehow prevent the proper formation of MV-H tetramer or its conformational shift upon receptor binding (Saphire and Oldstone, 2011). The similar experiment with the NDV-HN protein did not affect its fusion-support activity (Mahon et al., 2008).

Two models have been proposed for fusion triggering in paramyxoviruses. In one model, the attachment protein undergoes a conformational change upon receptor binding. This conformational change directly affects the F protein, causing its refolding which in turn drives membrane fusion. This model is consistent with the data for viruses using sialic acid as a receptor. In cells infected with hPIV3 and PIV5, the HN protein is associated with the F protein on the cell surface, but not in the endoplasmic reticulum (ER) (Paterson et al., 1997). Furthermore, the increased strength of the HN-F interaction enhances fusion activity. These results suggest that upon receptor binding, HN actively acts on the F protein and facilitates its refolding (Connolly et al., 2009). In the second model, the attachment protein serves as a clamp that stabilizes the F protein in its pre-fusion state. Receptor binding of the attachment protein releases the F protein from the clamp to facilitate its spontaneous conformational change. MV entry is consistent with this model. MV-H is already associated with MV-F within the ER (Plemper et al., 2001), and the conformational shift of the tetramer is likely to facilitate the release of MV-F from the heteromeric H–F oligomers. This release model is also supported by the data that a weaker interaction between MV-H and MV-F results in increased fusogenicity (Plemper et al., 2002; Corey and Iorio, 2009). A similar release model has also been proposed for NiV and HeV (Aguilar et al., 2006, 2007; Bishop et al., 2007). Thus, different paramyxoviruses may use different mechanisms of fusion triggering, although the overall cell entry mechanism may be similar among them.

STRUCTURAL INSIGHT INTO MV SEROTYPE AND VACCINE

Crystal structure of MV-H sheds light on why measles vaccine has been successful for a long time (Hashiguchi et al., 2007, 2011; Ruigrok and Gerlier, 2007). The structure suggests that N-linked sugars (at positions 168, 187, 200, and 215) on MV-H cover a considerable portion of its surface, only exposing a small area for receptor and antibody bindings (**Figures 2A,B**). Indeed, crystal structures of MV-H–SLAM and MV-H–CD46 complexes indicate that both receptors target this exposed area. Mutagenesis studies have also revealed that nectin-4 binds to this region as well. Furthermore, a majority of MV-H monoclonal antibodies are mapped onto this exposed receptor-binding area, indicating that this area acts as the epitope "hot spot." This overlap of binding sites for receptors and neutralizing antibodies explains why measles vaccine, derived from a single strain, remains effective against all 23 distinct MV genotypes. A functional importance (receptor binding) likely exerts a restrain that renders this region highly unfavorable to mutation. As a result, MV still occurs in